6. Yannuzzi LA, Wong DW, Sforzolini BS, et al. Polypoidal choroidal vasculopathy and neovascularized age-related macular degeneration. Arch Ophthalmol 1999;117:1503–10.
7. Uyama M, Matsubara T, Fukushima I, et al. Idiopathic polypoidal choroidal vasculopathy in Japanese patients. Arch Ophthalmol 1999;117:1035–42.
8. Liu Y, Wen F, Huang S, et al. Subtype lesions of neovascular age-related macular degeneration in Chinese patients. Graefes Arch Clin Exp Ophthalmol 2007;245:1441–5.
9. Maruko I, Iida T, Saito M, et al. Clinical characteristics of exudative age-related macular degeneration in Japanese patients. Am J Ophthalmol 2007;144:15–22.
10. Laude A, Cackett PD, Vithana EN, et al. Polypoidal choroidal vasculopathy and neovascular age-related macular degeneration: same or different disease? Prog Retin Eye Res 2010;29:19–29.
11. Dandekar SS, Jenkins SA, Peto T, et al. Autofluorescence imaging of choroidal neovascularization due to age-related macular degeneration. Arch Ophthalmol 2005;123:1507–13.
12. McBain VA, Townend J, Lois N. Fundus autofluorescence in exudative age-related macular degeneration. Br J Ophthalmol 2007;91:491–6.
13. Vaclavik V, Vujosevic S, Dandekar SS, et al. Autofluorescence imaging in age-related macular degeneration complicated by choroidal neovascularization: a prospective study. Ophthalmology 2008;115:342–6.
14. Lafaut BA, Bartz-Schmidt KU, Vanden Broecke C, et al. Clinicopathological correlation in exudative age related macular degeneration: histological differentiation between classic and occult choroidal neovascularisation. Br J Ophthalmol 2000;84:239–43.
15. Iijima H, Iida T, Imai M, et al. Optical coherence tomography of orange-red subretinal lesions in eyes with idiopathic polypoidal choroidal vasculopathy. Am J Ophthalmol 2000;129:21–6.
16. Tateiwa H, Kuroiwa S, Gaun S, et al. Polypoidal choroidal vasculopathy with large vascular network. Graefes Arch Clin Exp Ophthalmol 2002;240:354–61.
17. Iijima H, Imai M, Gohdo T, Tsukahara S. Optical coherence tomography of idiopathic polypoidal choroidal vasculopathy. Am J Ophthalmol 1999;127:301–5.
18. Ojima Y, Hangai M, Sakamoto A, et al. Improved visualization of polypoidal choroidal vasculopathy lesions using spectral-domain optical coherence tomography. Retina 2009;29:52–9.
19. Sato T, Kishi S, Watanabe G, et al. Tomographic features of branching vascular networks in polypoidal choroidal vasculopathy. Retina 2007;27:589–94.
20. Ueta T, Iriyama A, Francis J, et al. Development of typical age-related macular degeneration and polypoidal choroidal vasculopathy in fellow eyes of Japanese patients with exudative age-related macular degeneration. Am J Ophthalmol 2008;146:96–101.
21. Sasahara M, Tsujikawa A, Musashi K, et al. Polypoidal choroidal vasculopathy with choroidal vascular hyperpermeability. Am J Ophthalmol 2006;142:601–7.
22. Imamura Y, Fujiwara T, Spaide RF. Fundus autofluorescence and visual acuity in central serous chorioretinopathy. Ophthalmology 2011;118:700–5.

Footnotes and Financial Disclosures

Originally received: November 18, 2011.
Final revision: January 13, 2012.
Accepted: February 9, 2012.
Available online: April 17, 2012. Manuscript no. 2011-1661.

Department of Ophthalmology, Kyoto Prefectural University of Medicine, Kyoto, Japan.

Presented in part at: the Association for Research in Vision and Ophthalmology Annual Meeting, May 2, 2011, Fort Lauderdale, Florida.

Financial Disclosure(s):
The author(s) have no proprietary or commercial interest in any materials discussed in this article.

Supported in part by Grant No. 22791676 from the Ministry of Education, Culture, Sports, Science and Technology-Japan (Dr. Koizumi).

Correspondence:
Hideki Koizumi, MD, PhD, Department of Ophthalmology, Kyoto Prefectural University of Medicine, 465 Kajii-cho, Kamigyo-ku, Kyoto 602-0841, Japan. E-mail: hidekoiz@koto.kpu-m.ac.jp.

*Drs. Yamagishi and Koizumi contributed equally as co–first authors.

The Maintenance of Lymphatic Vessels in the Cornea Is Dependent on the Presence of Macrophages

Kazuichi Maruyama,[1-3] *Toru Nakazawa,*[4] *Claus Cursiefen,*[5] *Yuko Maruyama,*[1] *Nico Van Rooijen,*[3] *Patricia A. D'Amore,*[2] *and Shigeru Kinoshita*[2]

Purpose. It has been shown previously that the presence in the cornea of antigen-presenting cells (APC), such as macrophages (MPS) and lymphangiogenesis, is a risk for corneal transplantation. We sought to determine whether the existence of lymphatic vessels in the non-inflamed cornea is associated with the presence of MPS.

Methods. Flat mounts were prepared from corneas of untreated C57BL/6, CD11b$^{-/-}$, F4/80$^{-/-}$, and BALB/c mice, and after suture placement or corneal transplantation, observed by immunofluorescence for the presence of lymphatic vessels using LYVE-1 as a marker of lymphatic endothelium. Innate immune cells were detected in normal mouse corneas using CD11b, F4/80, CD40, as well as MHC-class II. Digital images of the flat mounts were taken using a spot image analysis system, and the area covered by lymphatic vessels was measured using NIH Image software.

Results. The number of spontaneous lymphatic vessels in C57BL/6 corneas was significantly greater than in BALB/c corneas ($P = 0.03$). There were more CD11b^{+} ($P < 0.01$) and CD40^{+}, MHC-class II (+) cells in the C57BL/6 corneas than in BALB/c mouse corneas. MPS depletion via clodronate liposome in C57BL/6 mice led to fewer spontaneous lymphatic vessels and reduced inflammation-induced lymphangiogenesis relative to control mice. Mice deficient in CD11b or F4/80 had fewer spontaneous lymphatic vessels and less lymphangiogenesis than control C57BL/6 mice.

Conclusions. C57BL/6 mouse corneas have more endogenous CD11b^{+} cells and lymphatic vessels. The endogenous lymphatic vessels, along with pro-inflammatory MPS, account for the high risk of corneal graft rejection in C57BL/6 mice. CD11b^{+} and F4/80^{+} MPS appear to have an important role in of the formation of new lymphatic vessels. (*Invest Ophthalmol Vis Sci.* 2012;53:3145-3153) DOI:10.1167/iovs.11-8010

From the [1]Department of Ophthalmology, Kyoto Prefectural University of Medicine, Kyoto, Japan; [2]The Schepens Eye Research Institute, Department of Ophthalmology, Harvard Medical School, Boston, Massachusetts; the [4]Department of Ophthalmology, Tohoku University School of Medicine, Sendai, Japan; the [5]Department of Ophthalmology, University of Cologne, Cologne, Germany; and the [3]Department of Molecular Cell Biology and Immunology, Faculty of Medicine, Free University, Amsterdam, The Netherlands.

Supported by Grant FY-2011 KAKEN 23592613.

Submitted for publication June 7, 2011; revised October 12, 2011 and January 31, 2012; accepted April 10, 2012.

Disclosure: **K. Maruyama**, None; **T. Nakazawa**, None; **C. Cursiefen**, None; **Y. Maruyama**, None; **N. Van Rooijen**, None; **P.A. D'Amore**, None; **S. Kinoshita**, None

Corresponding author: Kazuichi Maruyama, Department of Ophthalmology, Kyoto Prefectural University of Medicine, 465 Kajii-cho Kamigyo-ku, Kyoto, Japan, 602-0841; telephone +81-75-251-5578; fax 81-75-251-5663; kmaruyam@koto.kpu-m.ac.jp.

Blood and lymphatic vessels are critical to organ and tissue maintenance. In particular, the lymphatic system is central to the tissue fluid homeostasis, and to the return of macromolecules and immune cells to the blood stream. However, some tissues, including the cornea, have neither vascular nor lymphatic vessels. The lack of a vascular supply is essential to maintaining the transparency of the cornea. The cornea obtains its nutrients by diffusion from the aqueous fluid and the tears. The mechanisms that underlie the avascularity of the cornea may be related to the immune-privilege of the eye.[1,2] In addition, the presence of anti-angiogenic factors, such as sFlt, VEGFR3, and thrombospondin-1, have been associated with avascularity of the cornea.[1-3]

The wound healing that follows corneal transplantation involves the growth of blood and lymphatic vessels as part of the acute inflammatory response. The lymphatics provide a route for the transport of antigens by antigen-presenting cells (APC) via the efferent pathway to the regional lymph node. After antigen presentation, activated T cells return to the cornea via the blood vessels, a process referred to as the afferent pathway.[4-6] Corneal transplantation in the absence of vascularization has the lowest rejection rates and graft survival approaches 90%.[7,8] In contrast, vascularized corneas have much higher rejection rates with survival below 50%.[8,9] It is well known that host C57BL/6 allo-corneal transplantations have a higher rejection rate than host BALB/c- allo corneal transplantations.[10] This difference in rejection rate can be explained, at least in part, by differential immunological responses between BALB/c and host C57BL/6 mouse strains.[11]

MPS and other innate immune cells (some expressing MHC-class II antigens) are present in the corneal epithelial layer and stroma,[12-16] especially in the peripheral cornea (limbus).[17] Following the induction of inflammation, MPS are activated and the expression of MHC-class II, as well as co-stimulatory molecules, such as CD80 (B7.1), CD86 (B7.2), and CD40, is increased.[17,18] We and others have found that activated MPS can contribute to lymphatic vessels in inflammation-associated lymphangiogenesis.[19-21] Based on these observations, we postulated that the differences in endogenous MPS might account for the observed difference in graft rejection rate.

Methods

Mouse Corneal Transplantation and Corneal Suture Placement Models

Male BALB/c and C57BL/6 mice (Taconic Farms, Germantown, NY and Crea Japan, Shizuoka, Japan), CD11b$^{-/-}$ (B6.129S7-*Ifng*^{tm1Ts}/J mice; The Jackson Laboratory, Bar Harbor, ME),[22] and F4/80$^{-/-}$[23] mice were used at 8-12 weeks of age. All animal protocols were approved by Schepens Animal Care and Use Committee, and the Committee for Animal Research of Kyoto Prefectural University of Medicine in accordance with the Association for Research in Vision and Ophthal-

mology (ARVO) Statement for the Use of Animals in Ophthalmic and Vision Research.

For the corneal transplantation, each animal was anesthetized by an intraperitoneal (IP) injection of 3 mg ketamine and 0.007 mg xylazine before the surgical procedure. The central 2-mm portion of the donor cornea was excised with Vannas scissors and secured in recipient graft beds with 8 interrupted 11-0 nylon sutures (MANI Inc, Tochigi, Japan).[24] For the suture placement, three 11-0 nylon sutures were placed intrastromally using stromal incursions that encompassed more than 120 degrees of the corneal circumference. To obtain a standardized angiogenic response, the outer edge of the suture was placed halfway between the limbus and the line outlined by the 2-mm trephine; the inner edge was equidistant from the 2-mm trephine. Sutures were left in place for seven days.

Whole-Mount Determination of Blood and Lymphatic Vessels

Mice were euthanized by CO_2 inhalation, and the corneas were excised, rinsed three times in PBS, and fixed in acetone for 1 hour. The corneas were rinsed once in PBS, blocked with 2% BSA containing PBS, and incubated with rabbit anti-mouse LYVE-1 antibody (1:200; a lymphatic endothelium-specific hyaluronic acid receptor; RELIATECH, Wolfenbüttel, Germany).[25,26] The corneas were washed, blocked, and stained with Cy3-conjugated secondary antibody (1:100; Jackson ImmunoResearch Laboratories, Westgrove, PA). For visualization, stained whole-mount corneas were viewed under a Zeiss Axiophot microscope, and a Leica TSC-SP2 inverted and an upright confocal laser-scanning microscope. Digital images of the flat mounts were taken using a spot image analysis system, and the area covered by lymphatic vessels positive for LYVE-1[25,26] was measured using NIH Image software. The total corneal area was outlined using the innermost vessel of the limbal arcade as the border; the area of lymphatic vessels within the cornea was calculated and normalized to the total corneal area. Results are expressed as a percentage of the cornea covered by vessels.

Whole-Mount Determination of CD11b Positive Cells

For the whole mount corneal staining, corneas were removed and fixed with acetone for 1 hour, then rinsed in PBS, blocked with 2% BSA containing PBS, incubated with FITC, PE-conjugated CD11b (BD-Pharmingen, San Diego, CA) or anti-mouse F4/80 (1:100). Rat (DA) IgG_{2b}, κ (1:100, BD Pharmingen) was used as an isotype control. Corneas then were washed, blocked, and stained with FITC or PE conjugated CD40 and MHC-class II (Ia^d; BALB/c, Ia^b; C57BL/6; BD-Pharmingen). Double-stained whole mount corneas were visualized and photographed as described above. The same laser status was used when taking pictures in BALB/c and C57BL/6 mouse cornea. $CD11b^+$ cells were counted 300 μ from the corneal margin for the entire circumference of the cornea (limbal area).

Systemic and Local Depletion of MPS Using Clodronate Liposomes

Systemic and local depletion of monocytes/MPS was accomplished as described previously.[27] Cl2MDP (clodronate; a gift of Roche Diagnostics GmbH, Mannheim, Germany) was injected via tail vein (200 μL) and into subconjunctival space (40 μL) of C57BL/6 mice three times in a week (days 0, 3, and 5). Control mice received liposomes containing PBS at the same time points.

Immunofluorescence Staining for F4/80, LYVE-1, and 4′,6-Diamidino-2-Phenylindole (DAPI)

After fixation with 4% paraformaldehyde (PFA) at 4°C for 24 hours, the corneas were washed three times with PBS, placed into Tissue-Tek, and frozen −80°C for 24 hours. Sections (4 μm) were fixed with 99% cold acetone for two minutes, washed three times with PBS, then blocked with 0.3% Triton-x100 and 2% BSA containing PBS for 30 minutes. The corneas were incubated with primary antisera rabbit anti-F4/80 (1:1000; Serotec, Oxford, UK), MHC class II (1:1000; eBioscience) or LYVE-1 overnight at 4°C, then washed, blocked and the secondary Cy3-conjugated donkey anti-rabbit (1:2500; Jackson ImmunoResearch, Westgrove, PA) or FITC-conjugated goat anti-rat (1:2500, Jackson ImmunoResearch) was added for 30 minutes, followed by washing. Then, the corneas were washed with PBS, and mounting with VECTASHIELD with DAPI (Vector, Burlingame, CA).

Results

Presence of Innate Immune Cells in the Inflamed Cornea

We demonstrated previously the development of lymphatic vessels in the cornea after transplantation.[19] At day three after transplantation, lymphatic vessels began to grow into corneal stroma. Corneal lymphangiogenesis has been shown to be associated with $CD11b^+$ MPS.[19] Therefore, we investigated the presence of MPS in cornea at day three after transplantation. We used the corneal transplantation model of inflammation to assess macrophage infiltration into corneal stroma. Three days after BALB/c syngeneic corneal transplantation (Fig. 1a), the mice were euthanized, and the corneas were dissected from the limbus, fixed, and stained with anti-CD11b-FITC conjugated antibody. In the naïve, non-transplanted cornea there was a small number of $CD11b^+$ cells, primarily in the limbal area (Fig. 1b). In contrast, inflamed corneas, such as after transplantation, contained large numbers of $CD11b^+$ cells (Fig. 1c). Similarly, sections of inflamed corneas revealed many MHC class II^+ cells (Fig. 1d). Moreover, some of the $F4/80^+$ cells expressed LYVE-1 and had aligned with lymphatic vessels (Fig. 1e).

Comparison of $CD11b^+$ in BALB/c and C57BL/6 Mouse Corneas

The presence in the corneal stroma of bone marrow-derived $CD11b^+$ MPS has been reported previously.[28] Quantification revealed significantly more $CD11b^+$ cells in C57BL/6 mouse corneas than in BALB/c mouse corneas ($P < 0.01$: C57BL/6 1439 ± 203SE, BALB/c 465 ± 74 SE). MHC class II^+ cells were located at limbal area under non-inflamed condition. As for $CD11b^+$ cells, the number of MHC class II^+ cells in C57BL/6 mice was higher than in BALB/c mice (Figs. 2a, b). Most of the $CD11b^+$ cells were in the stromal layer of the limbus. These cells also expressed CD40 and MHC-class II marker (Fig. 2c). There was a relatively small number of CD40 expressing cells in BALB/c mice corneas (data not shown). These results indicate that C57BL/6 mouse corneas have higher numbers of endogenous activated (MHC class II and CD40 +) $CD11b^+$ cells than BALB/c mouse corneas, suggesting a low level of chronic MPS activation in the limbal areas of C57BL/6 mice.

Comparison of Blood and Lymphatic Vessels in Naive BALB/C and C57BL/6 Mouse Corneas

It has been reported previously that the lymphangiogenic response in the cornea is strain-dependent.[29] In addition, the presence of spontaneous lymphatic vessels has been demonstrated in normal mouse cornea.[30] Although the cornea generally is considered to be devoid of blood and lymphatic vessels (Figs. 3a, b), the use of appropriate markers (LYVE-1) revealed lymphatic vessels (Figs. 3c, e) in the corneal stroma of

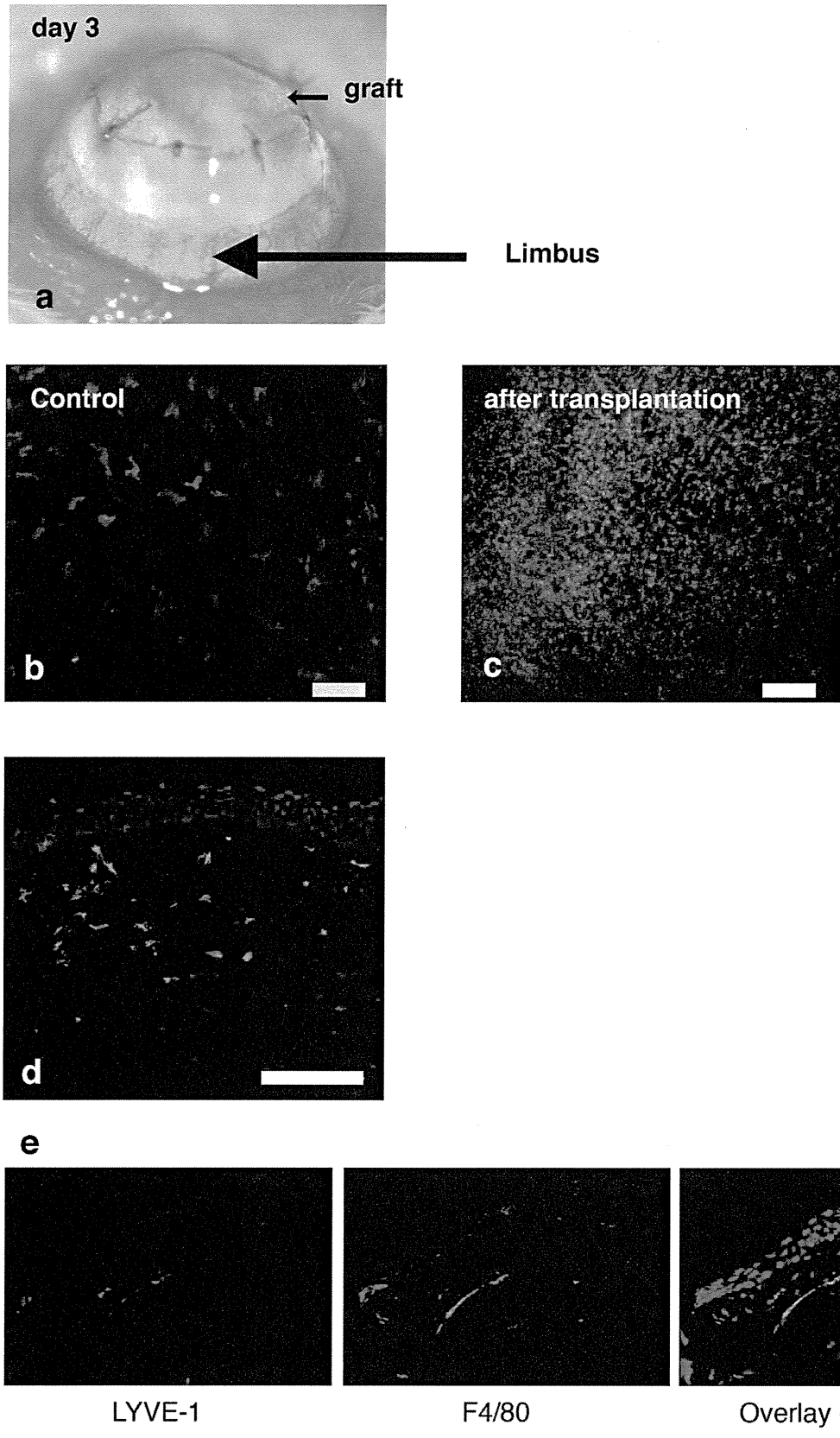

Figure 1. Macrophage and MHC class II+ cell density in the cornea. (**a**) Microscopic image, and (**b**, **c**) flat mounts of corneas stained for the presence of CD11b (+) cells. (**b**) Normal BALB/c corneal limbus and (**c**) host BALB/c corneal limbus on day 3 after corneal transplantation. Scale bar is 80 μm. (**d**) Section of limbus at day 3 after corneal transplantation. *Green label* (FITC) indicated MHC class II staining, *blue label* indicates DAPI staining. Scale bar is 150 μm. (**e**) Corneal lymphatic vessels at the limbal cornea stained with LYVE-1 (*red*), F4/80 (*green*), and DAPI (*blue*). Scale bar is 150 μm.

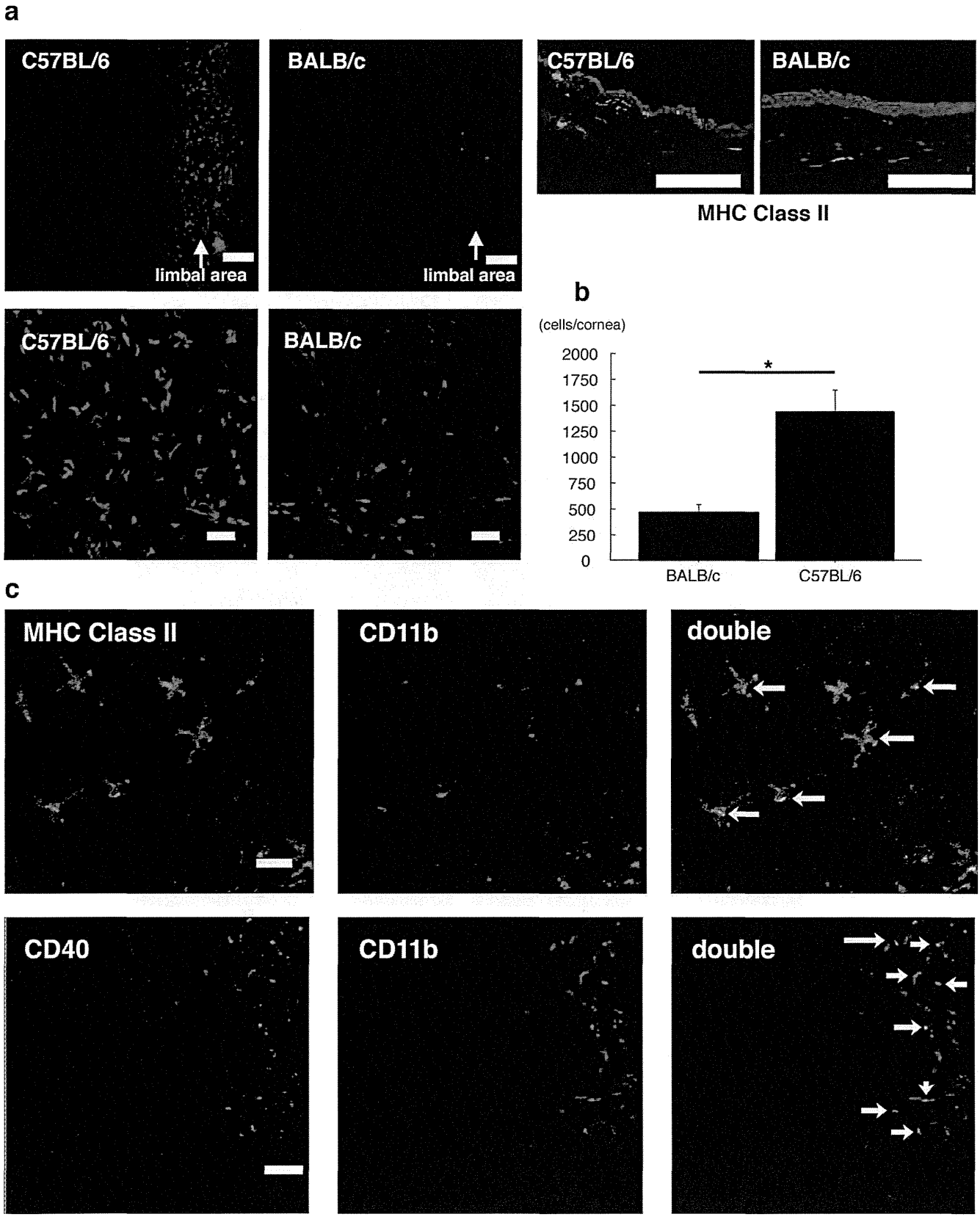

FIGURE 2. Comparison of CD11b (+) cell density in C57BL/6 and BALB/c mouse corneas. (**a**) Whole mount staining of the corneal limbus of normal C57BL/6 and BALB/c mouse, higher magnification of corneal limbus in normal C57BL/6 and BALB/c mouse. Sections of limbus of normal C57BL/6 and BALB/c mouse. *Green label* (FITC) indicates MHC class II staining, *blue label* indicates DAPI staining. (**b**) Comparison of CD11b + cell density between normal C57BL/6 and BALB/c mice (*$P < 0.05$). (**c**) Corneal limbus of C57BL/6; MHC-class II (*green*), CD11b, overlay of (MHC-class II), and (CD11b), CD40 (*green*), CD11b (*red*), overlay of (CD40), and (CD11b). Scale bars are: (**a**) top 2 figures, 80 μm; (**a**) lower 2 figures, 20 μm; sections, 150 μm; (**c**) 40 μm.

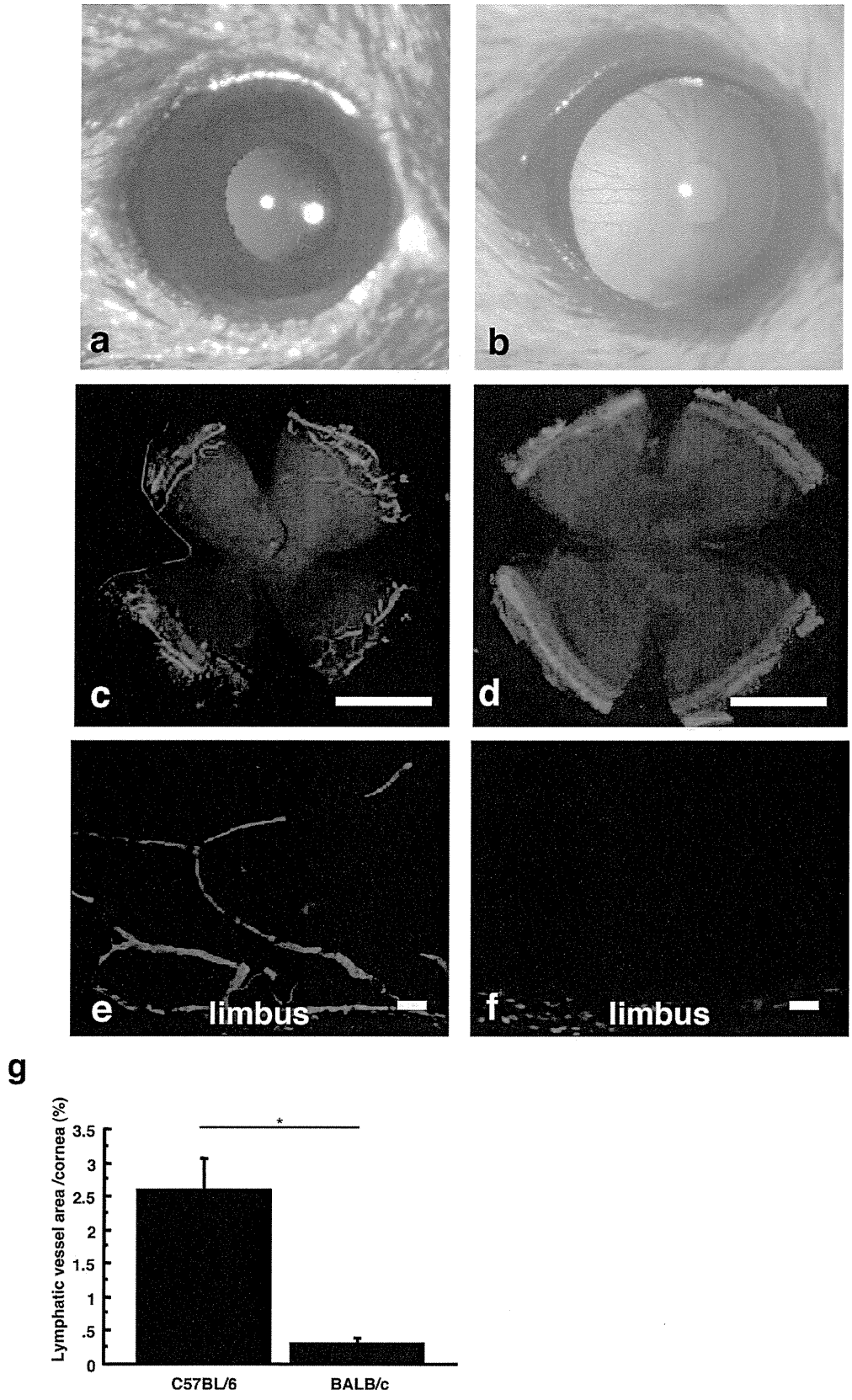

Figure 3. Comparison of lymphatic vessel area in corneal limbus between C57BL/6 and BALB/c mice. (**a**) Normal C57BL/6 mouse. (**b**) Normal BALB/c cornea. (**c**, **e**) LYVE-1 labeling of lymphatic vessels (*red*) in C57BL/6 cornea. (**d**, **f**) LYVE-1 labeling of lymphatic vessels in BALB/c cornea. (**g**) Comparison of lymphatic vessel area in corneal limbus between C57BL/6 and BALB/c mice ($P = 0.03$, $n = 5$). Scale bars are (**c**, **d**) 1 mm and (**e**, **f**) 100 μm.

6–8-week-old naïve C57BL/6 mice. In contrast, BALB/c mice (Figs. 3d, f), which are "low responders" for lymphatic vessel formation, had significantly fewer lymphatic vessels in cornea (Fig. 3g, $^*P = 0.03$).

The Effect of MPS Depletion on Lymphangiogenesis in C57BL/6 Mouse

We showed previously that clodronate depletion of MPS leads to reduced lymphangiogenesis in the inflamed cornea.[19] However, to our knowledge the effect of MPS depletion on the non-inflamed cornea has not been investigated. Above, we described the presence of activated MPS expressing CD40 or MHC-class II in C57BL/6 mouse cornea. We, therefore, sought to determine whether clodronate deletion of MPS in C57BL/6 corneal stroma would influence the presence of the endogenous lymphatic vessels. Systemic and local clodronate treatment reduced the number of endogenous lymphatic vessel structures in C57BL/6 mice. Some of the lymphatic vessels were seen to be separate from limbal lymphatic vessels (Figs. 4a, b; $P < 0.05$). Moreover, clodronate treatment also led to fewer $CD11b^+$ cells in lymphatic vessels (some of the $CD11b^+$ cells expressed both CD11b and LYVE-1) in C57BL/6 mouse cornea, compared to the untreated corneas (Fig. 4c). These results suggested that activated endogenous MPS contributed to the lymphatic vessels seen in C57BL/6 mouse corneas.

Spontaneous Lymphatic Vessel and Lymphangiogenesis in $CD11b^{-/-}$ and $F4/80^{-/-}$ Mice

$CD11b^{-/-}$ mice have been reported to exhibit impaired corneal wound healing under inflammatory conditions.[31] However, the possible role of endogenous corneal lymphatic vessels and lymphangiogenesis has not been investigated to our knowledge. Examination of corneas from $CD11b^{-/-}$ and $F4/80^{-/-}$ mice revealed that the area of endogenous lymphatic vessels was smaller in $CD11b^{-/-}$ and $F4/80^{-/-}$ mice than in control C57BL/6 mice (Fig. 5a). Using the corneal suture model of inflammation to assess lymphangiogenesis in $CD11b^{-/-}$, $F4/80^{-/-}$, and wild C57BL/6 mice, we found that the extent of lymphangiogenesis in $CD11b^{-/-}$ and $F4/80^{-/-}$ mice corneas was less than in wild type mice (Fig. 5b). These results indicated that $F4/80^+$ or $CD11b^+$ cells are important for maintenance of the endogenous lymphatic vessels and for the process of lymphangiogenesis in the cornea.

Discussion

The cornea is one of the few tissues devoid of blood and lymphatic vessels. However, our results indicated the presence of lymphatic vessels in the corneal stroma, particularly in the limbal area. The endogenous lymphatic vessels were especially prominent in C57BL/6 mice, but were not detected in corneas of BALB/c, nor were they seen in corneas of $F4/80^{-/-}$ or $CD11b^{-/-}$ mice, which have low functional MPS. We demonstrated previously that the formation of lymphatic vessels in the cornea correlates well with the number of activated $CD11b^+$ MPS.[19] Furthermore, we have shown that under inflammatory conditions $CD11b^+$ MPS secrete the VEGF-A and VEGF-C.[32] Elimination of these cells by treatment with clodronate liposomes led to the suppression of inflammation-induced corneal hem- and lymphangiogenesis to levels less than control mice.[32]

Host C57BL/6 mice are known to have a higher rejection rate after allogeneic corneal transplantation than host BALB/c mice (50% for C57BL/6 to BALB/c, and 80% for BALB/c to C57BL/6).[11] However, the reason for this difference is not well understood. One possible explanation is the presence of some, as yet unidentified, class II^+ cells in the cornea whose number or immunogenicity differ between these two strains of mice. Alternatively, the two species might have the same number of these cells, but the frequency of their migration from the eye to the lymph node could be different.[11] Our data support the former explanation and demonstrated that C57BL/6 mice have a higher risk of corneal transplantation rejection because they contain relatively large numbers of activated $CD11b^+$ cell and lymphatic vessels compared to BALB/c mice. The larger number of $CD11b^+$ or MHC class II^+ cells in C57BL/6 mouse cornea would result in a more rapid and effective detection of alloantigens than in BALB/c mice.

The involvement of these cells in the rejection reaction is supported by the fact that MPS depletion via clodronate liposomes led to a decrease in rejection[33] and a suppression of inflammation-induced lymphangiogenesis.[32] Mice depleted of MPS by clodronate treatment exhibit no alloantigen tolerance and delayed type hypersensitivity is not suppressed.[33] In naïve (non-inflamed) corneas, intravenous/subconjunctival clodronate liposome injection led to a reduced number of lymphatic vessels and $CD11b^+$ cells in the C57BL/6 corneal stroma, suggesting that $CD11b^+$ cell may contribute to the maintenance of lymphatic vessels in these mice.

The role of MPS as a source of cytokines and growth factors, and as a phagocyte during wound healing, has been well documented.[34] We showed previously that MPS have a key role in the induction of lymphatic vessels under pathological conditions in cornea and skin. Some of the MPS that express lymphatic-specific markers, such as LYVE-1, podoplanin, and prox-1 contributed to the formation of lymphatic vessels.[19,35] In addition, we observed that MPS formed lymphatic vessel-like tubes in vitro in a density-dependent manner.[19] Accordingly, the lower number of MPS appeared to contribute to the reduced formation of lymphatic structures in the granulation tissue of wounds under diabetic conditions.[35]

The precise role of $CD11b^+$ cells during inflammation is not well understood. MPS express F4/80 and CD11b. F4/80 is a prototypic MPS membrane glycoprotein that is highly restricted to mature resident MPS subpopulations.[36] $F4/80^{-/-}$ mice do not display any apparent abnormality, indicating that F4/80 is dispensable for the development of mouse tissue MPS. However, a functional requirement for F4/80 in the production of TNF-alpha, IL-12 and IFN-gamma after exposure of the mouse spleen cells to *Listeria* has been demonstrated.[37] Thus, we speculate that F4/80 may function under pathological conditions. Also, CD11b is the alpha subunit of the predominant beta2 integrin expressed on monocyte/MPS. CD11b mediates many functions of myeloid cell, including adhesion, migration, chemotaxis, and phagocytosis.[38] Neutralization of CD11b using antibodies reduced the leukocyte recruitment under inflammatory conditions.[39] Consistent with this concept, the delay of corneal wound healing in $CD11b^{-/-}$ mouse might be mediated by dysfunction or reduced recruitment of monocyte/MPS.[31] We have shown that MPS infiltration (accumulation) into an inflamed site is important for the induction of lymphangiogenesis.[35] The reduced accumulation of MPS in $CD11b^{-/-}$ and $F4/80^{-/-}$ mice, resulting in fewer lymphatic vessels than wild type, is consistent with this observation, Our data indicate that endogenous lymphatic vessels in the corneas are maintained by activated MPS and, thus, we speculate that the number of MPS and lymphatic vessels in C57BL/6 mouse corneal limbus might contribute to the observed differences in graft rejection between C45BL/6 mice and BALB/c mice. In addition, it is likely that polymorphisms, epigenetic changes, and/or other systemic processes also may influence graft rejection in humans, and any of these may provide targets for future therapeutic modulation.

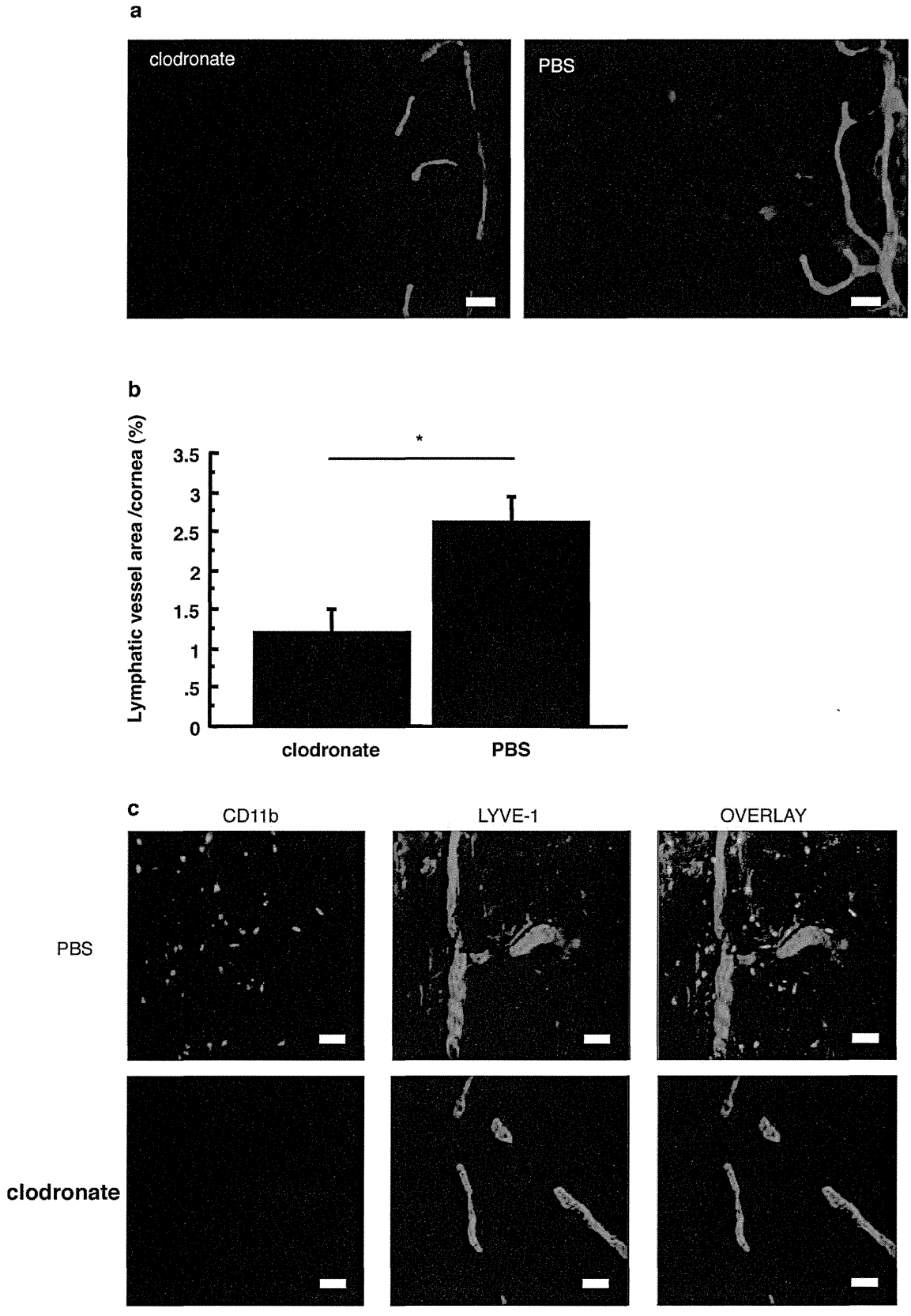

Figure 4. The effect of macrophage depletion on lymphangiogenesis in C57BL/6 mouse cornea. (**a**) Immunofluorescence of C57BL/6 mouse corneal flat mounts following clodronate liposome treatment and PBS liposome treatment. (**b**) Comparison of lymphatic vessel area in corneal limbus following clodronate and PBS liposome treatment (*$P < 0.05$). (**c**) LYVE-1 (*red*) and CD11b (*green*) immunofluorescent double labeling of corneas following clodronate or PBS liposome treatment. Scale bars are (**a**) 100 μm and (**c**) 40 μm.

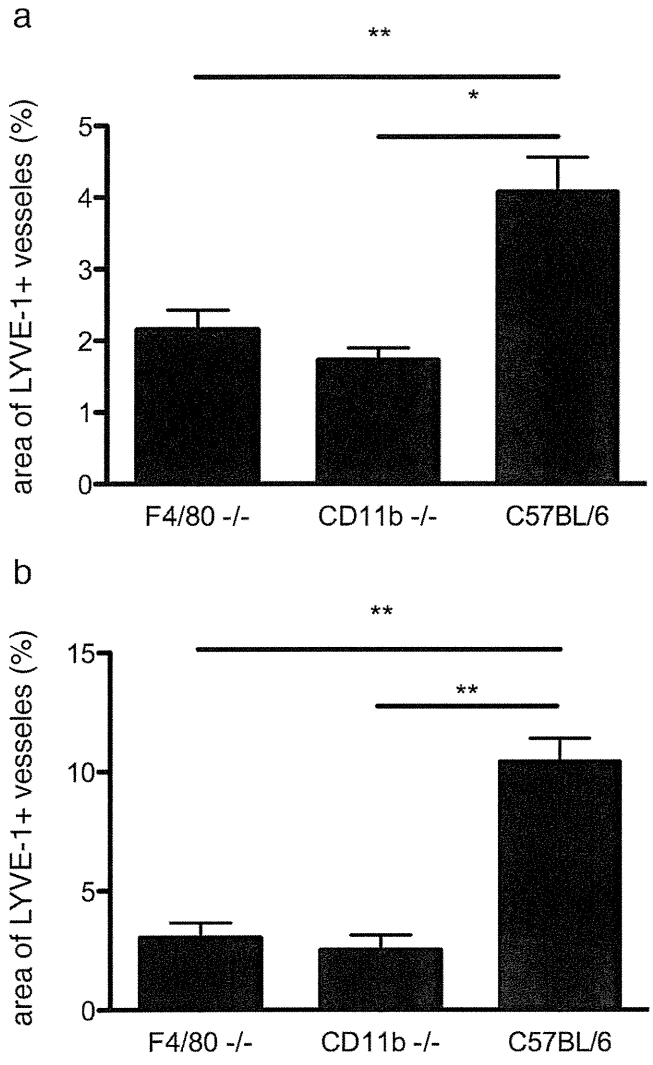

FIGURE 5. Endogenous lymphatic vessels and lymphangiogenesis in F4/80$^{-/-}$ and CD11b$^{-/-}$ mouse corneas. Quantification of (**a**) spontaneous lymphatic vessels $^{*}P = 0.0061$, $^{**}P = 0.0051$, no significant difference between F4/80$^{-/-}$ and CD11b$^{-/-}$, $n = 5$. (**b**) Lymphangiogenesis at day seven after suture placement, $^{**}P = 0.0095$, no significant difference between F4/80$^{-/-}$ and CD11b$^{-/-}$, $n = 5$.

Acknowledgments

His-Hsien Lin provided the F4/80$^{-/-}$ mice that were critical to our studies.

References

1. Ambati BK, Nozaki M, Singh N, et al. Corneal avascularity is due to soluble VEGF receptor-1. *Nature*. 2006;443:993-997.
2. Cursiefen C, Chen L, Saint-Geniez M, et al. Nonvascular VEGF receptor 3 expression by corneal epithelium maintains avascularity and vision. *Proc Natl Acad Sci U S A*. 2006;103:11405-11410.
3. Sekiyama E, Nakamura T, Cooper LJ, et al. Unique distribution of thrombospondin-1 in human ocular surface epithelium. *Invest Ophthalmol Vis Sci*. 2006;47:1352-1358.
4. Cursiefen C, Chen L, Dana MR, Streilein JW. Corneal lymphangiogenesis: evidence, mechanisms, and implications for corneal transplant immunology. *Cornea*. 2003;22:273-281.
5. Streilein JW, Bradley D, Sano Y, Sonoda Y. Immunosuppressive properties of tissues obtained from eyes with experimentally manipulated corneas. *Invest Ophthalmol Vis Sci*. 1996;37:413-424.
6. Streilein JW. Ocular immune privilege: therapeutic opportunities from an experiment of nature. *Nat Rev Immunol*. 2003;3:879-889.
7. Küchle M, Cursiefen C, Nguyen NX, et al. Risk factors for corneal allograft rejection: intermediate results of a prospective normal-risk keratoplasty study. *Graefes Arch Clin Exp Ophthalmol*. 2002;240:580-584.
8. Streilein JW, Yamada J, Dana MR, Ksander BR. Anterior chamber-associated immune deviation, ocular immune privilege, and orthotopic corneal allografts. *Transplant Proc*. 1999;31:1472-1475.
9. Maguire MG, Stark WJ, Gottsch JD, et al. Risk factors for corneal graft failure and rejection in the collaborative corneal transplantation studies. Collaborative Corneal Transplantation Studies Research Group. *Ophthalmology*. 1994;101:1536-1547.
10. Yamada J, Streilein JW. Fate of orthotopic corneal allografts in C57BL/6 mice. *Transpl Immunol*. 1998;6:161-168.
11. Yamada J, Ksander BR, Streilein JW. Cytotoxic T cells play no essential role in acute rejection of orthotopic corneal allografts in mice. *Invest Ophthalmol Vis Sci*. 2001;42:386-392.
12. Knickelbein JE, Watkins SC, McMenamin PG, Hendricks RL. Stratification of antigen-presenting cells within the normal cornea. *Ophthalmol Eye Dis*. 2009;1:45-54.
13. Chinnery HR, Humphries T, Clare A, et al. Turnover of bone marrow-derived cells in the irradiated mouse cornea. *Immunology*. 2008;125:541-548.
14. Chinnery HR, Pearlman E, McMenamin PG. Cutting edge: membrane nanotubes in vivo: a feature of MHC class II+ cells in the mouse cornea. *J Immunol*. 2008;180:5779-5783.
15. Xu H, Chen M, Reid DM, Forrester JV. LYVE-1-positive macrophages are present in normal murine eyes. *Invest Ophthalmol Vis Sci*. 2007;48:2162-2171.
16. Sosnova M, Bradl M, Forrester JV. CD34+ corneal stromal cells are bone marrow-derived and express hemopoietic stem cell markers. *Stem Cells*. 2005;23:507-515.
17. Hamrah P, Zhang Q, Liu Y, Dana MR. Novel characterization of MHC class II-negative population of resident corneal Langerhans cell-type dendritic cells. *Invest Ophthalmol Vis Sci*. 2002;43:639-646.
18. Qian Y, Dana MR. Effect of locally administered anti-CD154 (CD40 ligand) monoclonal antibody on survival of allogeneic corneal transplants. *Cornea*. 2002;21:592-597.
19. Maruyama K, Ii M, Cursiefen C, et al. Inflammation-induced lymphangiogenesis in the cornea arises from CD11b-positive macrophages. *J Clin Invest*. 2005;115:2363-2372.
20. Kerjaschki D, Huttary N, Raab I, et al. Lymphatic endothelial progenitor cells contribute to de novo lymphangiogenesis in human renal transplants. *Nat Med*. 2006;12:230-234.
21. Kataru RP, Jung K, Jang C, et al. Critical role of CD11b+ macrophages and VEGF in inflammatory lymphangiogenesis, antigen clearance, and inflammation resolution. *Blood*. 2009;113:5650-5659.
22. Lu H, Smith CW, Perrard J, et al. LFA-1 is sufficient in mediating neutrophil emigration in Mac-1-deficient mice. *J Clin Invest*. 1997;99:1340-1350.
23. Lin HH, Faunce DE, Stacey M, et al. The macrophage F4/80 receptor is required for the induction of antigen-specific efferent regulatory T cells in peripheral tolerance. *J Exp Med*. 2005;201:1615-1625.
24. Sonoda Y, Streilein JW. Orthotopic corneal transplantation in mice—evidence that the immunogenetic rules of rejection do not apply. *Transplantation*. 1992;54:694-704.

25. Cursiefen C, Schlötzer-Schrehardt U, Küchle M, et al. Lymphatic vessels in vascularized human corneas: immunohistochemical investigation using LYVE-1 and podoplanin. *Invest Ophthalmol Vis Sci.* 2002;43:2127–2135.
26. Chang L, Kaipainen A, Folkman J. Lymphangiogenesis new mechanisms. *Ann N Y Acad Sci.* 2002;979:111–119.
27. Ambati J, Anand A, Fernandez S, et al. An animal model of age-related macular degeneration in senescent Ccl-2- or Ccr-2-deficient mice. *Nat Med.* 2003;9:1390–1397.
28. Hamrah P, Liu Y, Zhang Q, Dana MR. The corneal stroma is endowed with a significant number of resident dendritic cells. *Invest Ophthalmol Vis Sci.* 2003;44:581–589.
29. Regenfuss B, Onderka J, Bock F, Hos D, Maruyama K, Cursiefen C. Genetic heterogeneity of lymphangiogenesis in different mouse strains. *Am J Pathol.* 177:501–510.
30. Nakao S, Maruyama K, Zandi S, et al. Lymphangiogenesis and angiogenesis: concurrence and/or dependence? Studies in inbred mouse strains. *FASEB J.* 24:504–513.
31. Li Z, Burns AR, Smith CW. Lymphocyte function-associated antigen-1-dependent inhibition of corneal wound healing. *Am J Pathol.* 2006;169:1590–1600.
32. Cursiefen C, Chen L, Borges LP, et al. VEGF-A stimulates lymphangiogenesis and hemangiogenesis in inflammatory neovascularization via macrophage recruitment. *J Clin Invest.* 2004;113:1040–1050.
33. Slegers TP, van der Gaag R, van Rooijen N, van Rij G, Streilein JW. Effect of local macrophage depletion on cellular immunity and tolerance evoked by corneal allografts. *Curr Eye Res.* 2003;26:73–79.
34. Singer AJ, Clark RA. Cutaneous wound healing. *N Engl J Med.* 1999;341:738–746.
35. Maruyama K, Asai J, Ii M, Thorne T, Losordo DW, D'Amore PA. Decreased macrophage number and activation lead to reduced lymphatic vessel formation and contribute to impaired diabetic wound healing. *Am J Pathol.* 2007;170:1178–1191.
36. Schaller E, Macfarlane AJ, Rupec RA, Gordon S, McKnight AJ, Pfeffer K. Inactivation of the F4/80 glycoprotein in the mouse germ line. *Mol Cell Biol.* 2002;22:8035–8043.
37. Warschkau H, Kiderlen AF. A monoclonal antibody directed against the murine macrophage surface molecule F4/80 modulates natural immune response to Listeria monocytogenes. *J Immunol.* 1999;163:3409–3416.
38. Arnaout MA. Structure and function of the leukocyte adhesion molecules CD11/CD18. *Blood.* 1990;75:1037–1050.
39. van Spriel AB, Leusen JH, van Egmond M, et al. Mac-1 (CD11b/CD18) is essential for Fc receptor-mediated neutrophil cytotoxicity and immunologic synapse formation. *Blood.* 2001;97:2478–2486.

Prostaglandin E2 Suppresses Poly I:C-Stimulated Cytokine Production Via EP2 and EP3 in Immortalized Human Corneal Epithelial Cells

Mayumi Ueta, MD, PhD,† Toshiyuki Matsuoka, MD, PhD,‡ Chie Sotozono, MD, PhD,* and Shigeru Kinoshita, MD, PhD**

Purpose: We previously reported that prostaglandin (PG) E_2 acts as a ligand for prostaglandin E receptor 3 (EP3) in conjunctival epithelial cells, that it downregulates the progression of experimental murine allergic conjunctivitis, and that in human conjunctival epithelial cells it modulates the expression of polyI:C-induced proinflammatory genes via prostaglandin E receptor 2 (EP2) and EP3, suggesting that PGE_2 might have important roles in ocular surface inflammation such as allergic conjunctivitis. Here, we investigated whether PGE_2 also downregulates polyI:C-induced cytokine production in human corneal epithelial cells.

Methods: We used enzyme-linked immunosorbent assay and quantitative reverse transcription–polymerase chain reaction to examine the effects of PGE_2 on polyI:C-induced cytokine expression by immortalized human corneal-limbal epithelial cells (HCLE). Using reverse transcription–polymerase chain reaction, we examined the messenger RNA (mRNA) expression of the PGE_2 receptor, EP1–4.

Results: PGE_2 significantly attenuated the expression of CC chemokine ligand (CCL)5 ($P < 0.0005$), CCL20 ($P < 0.0005$), C-X-C chemokine (CXCL)10 ($P < 0.0005$), CXCL11 ($P < 0.05$), and interleukin (IL)-6 ($P < 0.005$) in human corneal-limbal epithelial cells. Human corneal epithelial cells manifested the mRNA expression of EP2, EP3, and EP4, but not EP1. The EP2 agonist significantly suppressed the polyI:C-induced expression of CCL5 ($P < 0.005$), CXCL10 ($P < 0.0005$), and CXCL11 ($P < 0.05$) but not of CCL20 and IL-6. The EP3 agonist significantly suppressed the expression of CCL5 ($P < 0.05$), CCL20 ($P < 0.005$), CXCL10 ($P < 0.0005$), CXCL11 ($P < 0.0005$), and IL-6 ($P < 0.005$). The EP4 agonist failed to suppress cytokine production induced by polyI:C stimulation.

Conclusions: Our results show that in human corneal epithelial cells, PGE_2 attenuated the mRNA expression and production of CCL5, CXCL10, and CXCL11 via both EP2 and EP3, and that the mRNA expression and production of CCL20 and IL-6 was attenuated only by EP3.

Key Words: prostaglandin E_2 (PGE_2), human corneal epithelial cells, prostaglandin E receptor 3, prostaglandin E receptor 2

(*Cornea* 2012;31:1294–1298)

Prostanoids are a group of lipid mediators that form in response to various stimuli. They include prostaglandin (PG)D_2, PGE_2, $PGF_{2\alpha}$, PGI_2, and thromboxane (TX)A_2. They are released extracellularly immediately after their synthesis, and they act by binding to a G protein–coupled rhodopsin-type receptor on the surface of target cells. There are 8 types of prostanoid receptors: the PGD receptor (DP), 4 subtypes of the PGE receptor (EP1, EP2, EP3, and EP4), the PGF receptor (FP), the PGI receptor (IP), and the TXA receptor (TP).[1]

PolyI:C, a synthetic double-stranded (ds)RNA, which mimics viral dsRNA, is the well-known ligand of Toll-like receptor 3.[2] We have reported that polyI:C stimulation induces the secretion of inflammatory cytokines such as interleukin (IL)-6, IL-8, type I interferon (IFN) such as IFN-β, IFN-inducible proteins such as C-X-C chemokine (CXCL)10 and CXCL11, and allergy-related proteins such as CC chemokine ligand (CCL)5 and thymic stromal lymphopoietin in human ocular surface epithelium, both corneal and conjunctival.[3–5] Moreover, we also reported that not only Toll-like receptor 3, but also cytoplasmic helicase proteins, RIG-I (retinoic acid–inducible protein I) and MDA5 (melanoma differentiation–associated gene 5) contribute to polyI:C-inducible responses in conjunctival epithelium.[6]

We previously reported that PGE_2 acts as a ligand for EP3 in conjunctival epithelial cells, that it downregulates the

Received for publication April 21, 2011; revision received October 15, 2011; accepted November 10, 2011.

From the *Department of Ophthalmology, Kyoto Prefectural University of Medicine, Kyoto, Japan; †Department of Research Center for Inflammation and Regenerative Medicine, Faculty of Life and Medical Sciences, Doshisha University, Kyoto, Japan; and ‡Department of Ophthalmology, Tenri Hospital, Nara, Japan.

Supported in part by grants-in-aid for scientific research from the Japanese Ministry of Health, Labour and Welfare, the Japanese Ministry of Education, Culture, Sports, Science and Technology, a research grant from the Kyoto Foundation for the Promotion of Medical Science, the Intramural Research Fund of Kyoto Prefectural University of Medicine, and a research grant from the Shimizu Foundation.

The work described in the present article was carried out in collaboration with Ono Pharmaceutical Co, Ltd, who supplied ONO-AE-259, ONO-AE-248, and ONO-AE-329 used in this study. The authors have no other competing financial interests.

The authors have no conflicts of interest to disclose.

Supplemental digital content is available for this article. Direct URL citations appear in the printed text and are provided in the HTML and PDF versions of this article on the journal's Web site (www.corneajrnl.com).

Reprints: Mayumi Ueta, Department of Ophthalmology, Kyoto Prefectural University of Medicine, 465 Kajii-cho, Hirokoji-agaru, Kawaramachi-dori, Kamigyo-ku, Kyoto 602-0841, Japan (e-mail: mueta@koto.kpu-m.ac.jp).

progression of experimental murine allergic conjunctivitis,[7] and that in human conjunctival epithelial cells it modulates the expression of polyI:C-induced proinflammatory genes via not only EP3 but also EP2,[8] suggesting that PGE_2 might have important roles in the ocular surface inflammation such as allergic conjunctivitis.

PGE_2 was reported to be produced during inflammatory responses and to suppress the production of cytokines and chemokines induced by lipopolysaccharide (LPS) stimulation in macrophages[9,10] and dendritic cells.[11] Elsewhere, we documented that human corneal and conjunctival epithelial cells produce cytokines such as IL-6, IL-8, and IFN-β in response to stimulation with polyI:C but not LPS.[3,12,13] In this study, we examined the expression of the PGE_2 receptors, EP1, EP2, EP3, and EP4, in human corneal epithelial cells and investigated whether polyI:C-induced cytokine production is downregulated by PGE_2 in these cells.

MATERIALS AND METHODS

Human Corneal Epithelial Cells

This study was approved by the Institutional Review Board of Kyoto Prefectural University of Medicine, Kyoto, Japan. All experimental procedures were conducted in accordance with the tenets set forth in the Declaration of Helsinki.

For reverse transcription–polymerase chain reaction (RT-PCR) assay, we obtained human corneal epithelial cells from corneal grafts of patients who had undergone corneal transplantation for bullous keratopathy. Immortalized human corneal-limbal epithelial cells (HCLE), a gift from Dr Irene K. Gipson, were cultured in low calcium–defined keratinocyte serum-free medium (Invitrogen, Carlsbad, CA) with defined growth-promoting additives that included insulin, epidermal and fibroblast growth factors, and 1% antibiotic–antimycotic solution. The cells were used after reaching 80% confluence.[7]

Reverse Transcription–Polymerase Chain Reaction

RT-PCR assay was as previously described.[7] Briefly, total RNA was isolated from HCLE and human corneal epithelium using the Qiagen RNeasy kit (Qiagen, Valencia, CA) according to the manufacturer's instructions. For the RT reaction, we used the SuperScript Preamplification kit (Invitrogen). Amplification was with DNA polymerase (Takara, Shiga, Japan) for 38 cycles at 94°C for 1 minute, annealing for 1 minute, and 72°C for 1 minute on a commercial PCR machine (GeneAmp; PE Applied Biosystems). The primers were as previously reported.[7] RNA integrity was assessed by electrophoresis in ethidium bromide–stained 1.5% agarose gels. We performed 2 separate experiments.

Enzyme-Linked Immunosorbent Assay

Protein production was confirmed by enzyme-linked immunosorbent assay (ELISA). The amount of IL-6, CCL5, CCL20, CXCL11, and CXCL10 released into the culture supernatant was determined by ELISA using the human CCL5, CCL20, CXCL11, CXCL10 DuoSet (R&D Systems Inc, Minneapolis, MN) or the OptEIA IL-6 set (BD Pharmingen, San Diego, CA).[4,7,14]

We performed 3 separate experiments, each being carried out in 6 wells per group.

Quantitative RT-PCR

Total RNA was isolated from HCLE using the RNeasy Mini kit (Qiagen) according to the manufacturer's instructions. The RT reaction was with the SuperScript Preamplification kit (Invitrogen). Quantitative RT-PCR was on an ABI-prism 7700 instrument (Applied Biosystems, Foster City, CA) using a previously described protocol.[4,7,14] The primers and probes were from Applied Biosystems [assay ID: CCL5 (Hs00174575), CCL20 (Hs01011368), CXCL10 (Hs00171042), CXCL11 (Hs00171138), IL-6 (Hs00174131), and human GAPDH (Hs 4326317E)]. For complementary DNA (cDNA) amplification, we performed PCR in a 25 μl total volume that contained a 1-μl cDNA template in 2× TaqMan universal PCR master mix (Applied Biosystems) at 50°C for 2 minutes and 95°C for 10 minutes, followed by 40 cycles at 95°C for 15 seconds and 60°C for 1 minute. The results were analyzed with sequence detection software (Applied Biosystems). The quantification data were normalized to the expression of the housekeeping gene *GAPDH*. We performed 3 separate experiments, each being carried out in 6 wells per group.

Data Analysis

Data are expressed as the mean ± SEM and were evaluated by Student t test using the Microsoft Excel software program.

RESULTS

PGE2 Downregulated the Production of Cytokines Induced by Poly I:C Stimulation

Using HCLE and ELISA, we examined whether PGE_2 downregulated the production of IL-6, IL-8, CCL5, CCL20, CXCL10, and CXCL11 induced by polyI:C stimulation in human corneal epithelial cells. HCLE were exposed to 10 μg/mL polyI:C and 100 μg/mL PGE_2 for 24 hours (ELISA) or 6 hours (quantitative RT-PCR). We found that PGE_2 significantly attenuated the production of CCL5, CCL20, CXCL10, CXCL11, and IL-6 (all, $P < 0.0005$) (Fig. 1A). Quantitative RT-PCR assay confirmed that the messenger RNA (mRNA) expression of CCL5, CCL20, CXCL10, CXCL11, and IL-6 (respectively, $P < 0.0005$, $P < 0.0005$, $P < 0.0005$, $P < 0.05$ and $P < 0.005$) was significantly downregulated by PGE_2 (Fig. 1B).

Human Corneal Epithelial Cells Expressed EP2-, EP3-, and EP4-Specific mRNA

We then performed RT-PCR to assay the mRNA expression of the PGE_2 receptors, EP1, EP2, EP3, and EP4, in human corneal epithelial cells. PCR products of expected

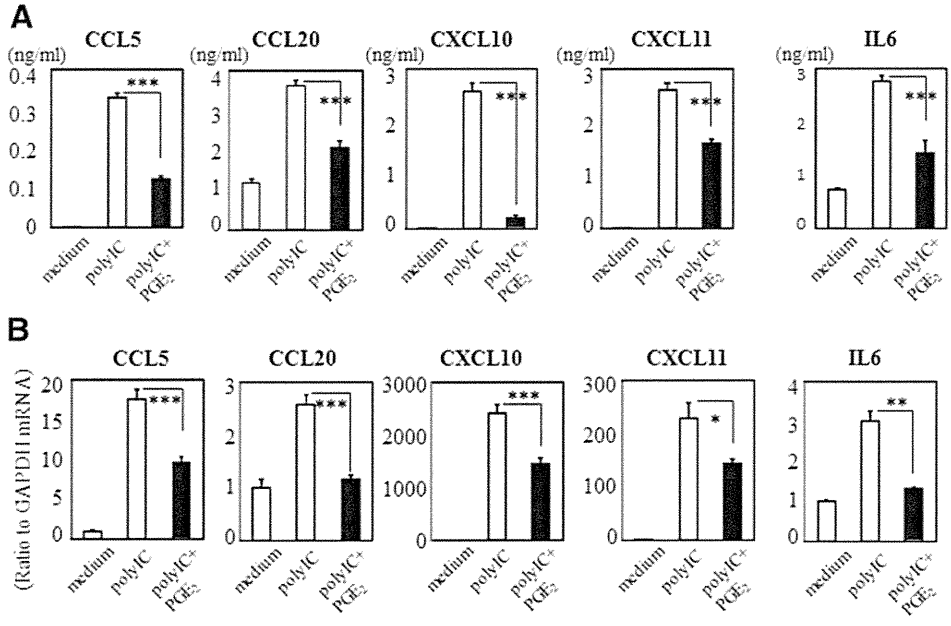

FIGURE 1. A, Suppression of the production of CCL5, CCl20, CXCL10, CXCL11, and IL-6 by PGE_2. HCLE were exposed to 10 μg/mL poly I:C and 100 μg/mL PGE_2 for 24 hours. Data are representative of 3 separate experiments and are given as the mean ± SEM from one experiment carried out in 6 wells per group. B, Suppression of mRNA expression of CCL5, CCL20, CXCL10, CXCL11, and IL-6 by PGE_2. HCLE were exposed to 10 μg/mL poly I:C and 100 μg/mL PGE_2 for 6 hours. The quantification data were normalized to the expression of the housekeeping gene *GAPDH*. The *y* axis shows the increase in specific mRNA over unstimulated samples. Data are representative of 3 separate experiments and are given as the mean ± SEM from one experiment carried out in 6 wells per group ($*P < 0.05$, $**P < 0.005$, $***P < 0.0005$).

lengths were obtained for EP2 (683 bp), EP3 (622 bp), and EP4 (956 bp) (Fig. 2), but not for EP1 (723 bp) (data not shown), from HCLE and *in vivo* human corneal epithelial cells, suggesting that the human corneal epithelium expresses EP2, EP3, and EP4 mRNAs. To confirm the specificity for the detection of EP2-, EP3-, and EP4 mRNA, we isolated and sequenced the PCR products. The obtained sequences were identical to the human EP2-, EP3-, and EP4 cDNA sequences. Moreover, we could detect EP2, EP3 and EP4 proteins using immunoblotting (see **Figure, Supplemental Digital Content 1**, http://links.lww.com/ICO/A42).

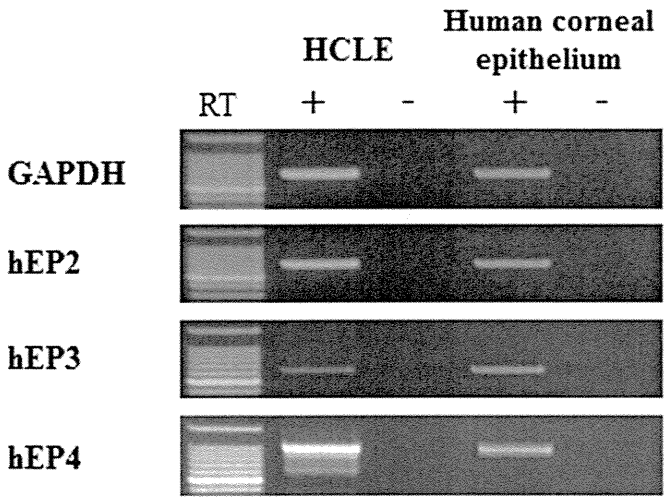

FIGURE 2. mRNA expression of the PGE_2 receptors EP2, EP3, and EP4. RT-PCR assay of the expression of PGE_2 receptor EP2, EP3, and EP4-specific mRNA in HLCE and human corneal epithelium. RT identifies data that were obtained without reverse transcription (controls).

EP2 and EP3, but not EP4 Agonists Downregulated the Production of Cytokines Induced by Poly I:C Stimulation

Using the EP2, EP3, and EP4 agonists, ONO-AE-259, ONO-AE-248, and ONO-AE-329, respectively, we also examined which PGE_2 receptor(s) contributed to their polyI:C-induced downregulation. HCLE were exposed to 10 μg/mL polyI:C and 10 μg/mL of the EP2, EP3, or EP4 agonist for 24 hours (ELISA) or 6 hours (quantitative RT-PCR). ELISA showed that the EP2 agonist significantly suppressed the polyI:C-induced production of CCL5, CXCL10, and CXCL11 (all, $P < 0.0005$) but not of CCL20 and IL-6, and that the EP3 agonist significantly suppressed the production of CCL5, CCL20, CXCL10, CXCL11, and IL-6 (all, $P < 0.0005$). However, the EP4 agonist failed to suppress the cytokine production induced by polyI:C stimulation (Fig. 3). Quantitative RT-PCR confirmed that the EP2 agonist significantly downregulated the mRNA expression of CCL5, CXCL10, and CXCL11 (respectively, $P < 0.005$, $P < 0.0005$ and $P < 0.05$), but not of CCL20 and IL-6, and that the EP3 agonist significantly downregulated the mRNA expression of all examined cytokines (CCL5, $P < 0.05$; CCL20, $P < 0.005$; CXCL10, $P < 0.0005$; CXCL11, $P < 0.0005$; and IL-6, $P < 0{,}005$) (Fig. 4). Thus, our results show that PGE_2 attenuated the mRNA expression and production of CCL5, CXCL10, and CXCL11 via both EP2 and EP3, and that the CCL20 and IL-6 mRNA expression and production were attenuated only by EP3 in human corneal epithelial cells.

DISCUSSION

Lipid mediators like PGE_2 regulate immune and inflammatory responses by modulating the production of cytokines and chemokines.[11] In macrophages, PGE_2 suppressed the proinflammatory gene expression induced by LPS,

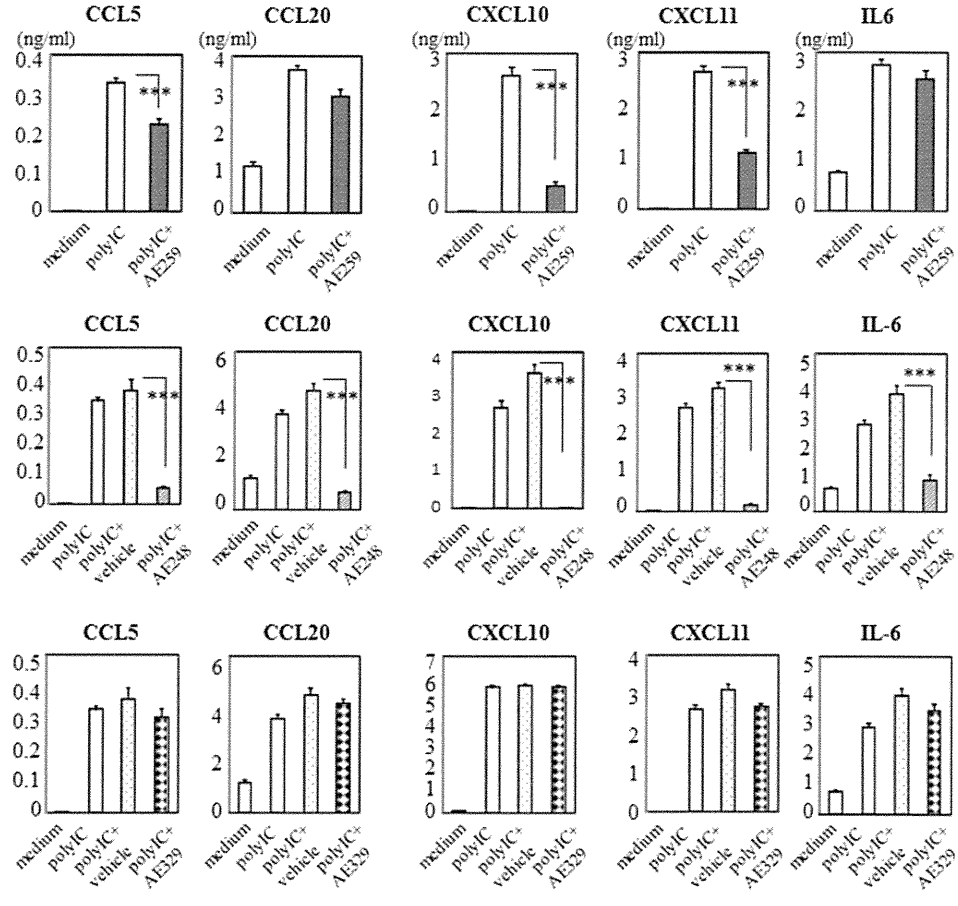

FIGURE 3. Effect of the PGE_2 receptors EP2, EP3, and EP4 on poly I:C-induced cytokine production. HCLE were exposed to 10 μg/mL poly I:C and 10 μg/mL EP2, EP3, or EP4 agonist for 24 hours. Data are representative of 3 separate experiments and are given as the mean ± SEM from one experiment carried out in 6 wells per group (***$P < 0.0005$).

including macrophage inflammatory protein (MIP)-1α, MIP-1β, CCL5, CXCL10, and IL-8.[9] Here we document that PGE_2 modulates the expression and production of polyI:C-induced proinflammatory genes in not only human conjunctival epithelial cells but also corneal epithelial cells. It exerted an inhibitory effect on polyI:C-induced CCL5, CCL20, CXCL10, CXCL11, and IL-6 mRNAs (respectively, $P < 0.0005$, $P < 0.0005$, $P < 0.0005$, $P < 0.05$ and $P < 0.005$) and on protein production in HCLE (all, $P < 0.0005$). PGE_2 exerts its biological actions by binding to EP located primarily on the plasma membrane. We confirmed the presence of the PGE_2 receptor subtypes, EP2,

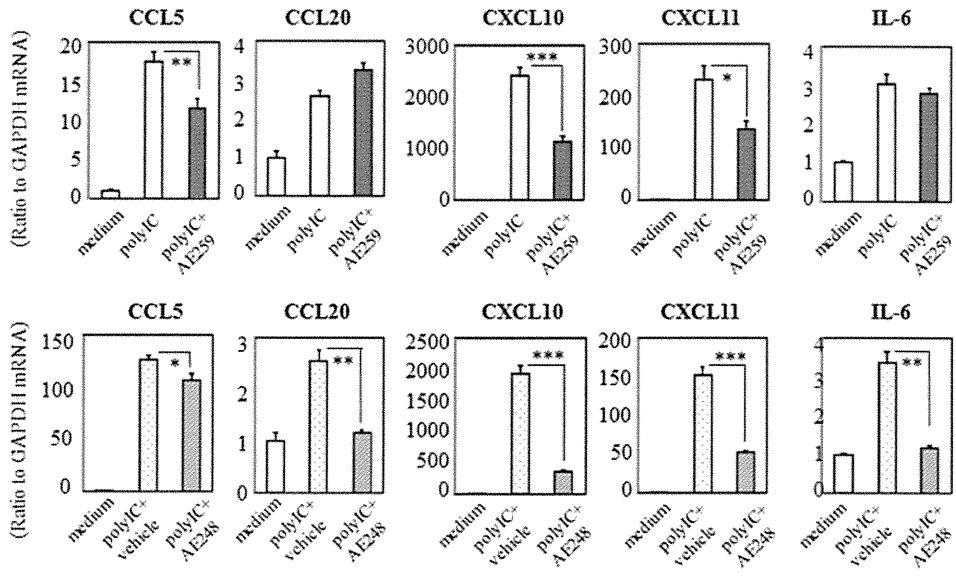

FIGURE 4. Effect of the PGE_2 receptors EP2 and EP3 on the poly I:C-induced mRNA expression of cytokines: HCLE were exposed to 10 μg/mL poly I:C and 10 μg/mL EP2 or EP3 agonist for 6 hours. The quantification data were normalized to the expression of the housekeeping gene *GAPDH*. The *y* axis shows the increase in specific mRNA over unstimulated samples. Data are representative of 3 separate experiments and are given as the mean ± SEM from one experiment carried out in 6 wells per group (*$P < 0.05$, **$P < 0.005$, ***$P < 0.0005$).

EP3, and EP4, in human corneal epithelial cells. Stimulation with either EP2- or EP3-specific agonists had a suppressive effect on polyI:C-induced CCL5, CXCL10, and CXCL11 production (both EP2- and EP3-specific agonists: all, $P < 0.0005$) , but only the EP3-specific agonist had a suppressive effect on the production of CCL20 and IL-6 (both, $P < 0.0005$).

Stimulation with PGE_2 exhibits immunosuppressive effects in various cell types including macrophages and dendritic cells via EP2 and/or EP4.[9–11] This phenomenon is explicable by the elevation of intracellular cyclic adenosine monophosphate (cAMP) via the activation of adenylcyclase.[9,10] Although PGE_2 acts on EP2 and EP4 and activates adenylcyclase, resulting in the elevation of intracellular cAMP, its action on EP3 suppresses adenylcyclase, resulting in a decrease in intracellular cAMP. In human conjunctival and corneal epithelial cells, both EP2 and EP3 contribute to the immunosuppressive effect against polyI:C stimulation; therefore, the suppressive effect cannot be explained by the elevation of intracellular cAMP. The precise molecular mechanisms underlying the immunosuppressive effects of PGE_2 in epithelial cells remain to be elucidated.

Release of PGE_2 is associated with ocular inflammation, but the exact role in inflammation has not been identified, rather PGE_2 might have been considered as inflammation-related molecules in the cornea. In this study, it is evident that PGE_2 could contribute to suppressing the production of various cytokines and chemokines in the ocular surface. Elsewhere we reported that PGE_2 acts as a ligand for EP3 in conjunctival epithelial cells and that it downregulates the progression of murine experimental allergic conjunctivitis,[7] suggesting the possibility of the PGE_2 and EP3 selective agonists as antiinflammatory drugs.

In summary, our results suggest that PGE_2 and its receptors in ocular surface (conjunctival and corneal) epithelium contribute to the regulation of ocular surface inflammation.

ACKNOWLEDGEMENTS

We thank Chikako Endo for technical assistance.

REFERENCES

1. Matsuoka T, Narumiya S. Prostaglandin receptor signaling in disease. *ScientificWorldJournal*. 2007;7:1329–1347.
2. Alexopoulou L, Holt AC, Medzhitov R, et al. Recognition of double-stranded RNA and activation of NF-kappaB by Toll-like receptor 3. *Nature*. 2001;413:732–738.
3. Ueta M, Kinoshita S. Ocular surface inflammation mediated by innate immunity. *Eye Contact Lens*. 2010;36:269–281.
4. Ueta M, Mizushima K, Yokoi N, et al. Gene-expression analysis of polyI:C-stimulated primary human conjunctival epithelial cells. *Br J Ophthalmol*. 2010;94:1528–1532.
5. Kumar A, Zhang J, Yu FS. Toll-like receptor 3 agonist poly(I:C)-induced antiviral response in human corneal epithelial cells. *Immunology*. 2006; 117:11–21.
6. Ueta M, Kawai T, Yokoi N, et al. Contribution of IPS-1 to polyI:C-induced cytokine production in conjunctival epithelial cells. *Biochem Biophys Res Commun*. 2011;404:419–423.
7. Ueta M, Matsuoka T, Narumiya S, et al. Prostaglandin E receptor subtype EP3 in conjunctival epithelium regulates late-phase reaction of experimental allergic conjunctivitis. *J Allergy Clin Immunol*. 2009;123:466–471.
8. Ueta M, Matsuoka T, Yokoi N, et al. Prostaglandin E2 suppresses polyinosine-polycytidylic acid (polyI:C)-stimulated cytokine production via prostaglandin E2 receptor (EP) 2 and 3 in human conjunctival epithelial cells. *Br J Ophthalmol*. 2011;95:859–863.
9. Takayama K, García-Cardena G, Sukhova GK, et al. Prostaglandin E2 suppresses chemokine production in human macrophages through the EP4 receptor. *J Biol Chem*. 2002;277:44147–44154.
10. Xu XJ, Reichner JS, Mastrofrancesco B, et al. Prostaglandin E2 suppresses lipopolysaccharide-stimulated IFN-beta production. *J Immunol*. 2008;180:2125–2131.
11. Shiraishi H, Yoshida H, Saeki K, et al. Prostaglandin E2 is a major soluble factor produced by stromal cells for preventing inflammatory cytokine production from dendritic cells. *Int Immunol*. 2008;20:1219–1229.
12. Ueta M, Hamuro J, Kiyono H, et al. Triggering of TLR3 by polyI:C in human corneal epithelial cells to induce inflammatory cytokines. *Biochem Biophys Res Commun*. 2005;331:285–294.
13. Ueta M, Kinoshita S. Innate immunity of the ocular surface. *Brain Res Bull*. 2010;81:219–228.
14. Ueta M, Sotozono C, Nakano M, et al. Association between prostaglandin E receptor 3 polymorphisms and Stevens-Johnson syndrome identified by means of a genome-wide association study. *J Allergy Clin Immunol*. 2010;126:1218–1225. e10.

CHOROIDAL THICKNESS IN INFERIOR STAPHYLOMA ASSOCIATED WITH POSTERIOR SEROUS RETINAL DETACHMENT

TETSUYA YAMAGISHI, MD, HIDEKI KOIZUMI, MD, PhD, TAIZO YAMAZAKI, MD, SHIGERU KINOSHITA, MD, PhD

Purpose: The purpose of the study was to describe the choroidal findings in eyes with posterior serous retinal detachment associated with inferior staphyloma by enhanced depth imaging optical coherence tomography.

Methods: The study involved five eyes of five patients with the inferior staphyloma accompanied by posterior serous retinal detachment. In each case, the upper border of the staphyloma was lying across the macula. Enhanced depth imaging spectral domain optical coherence tomography was performed in a vertical–sectional manner through the fovea, and the choroidal thicknesses at the thinnest point, at the fovea, and at 0.5 mm and 1.0 mm superior and inferior to the thinnest point were measured. Fluorescein angiography and indocyanine green angiography were also performed.

Results: In all 5 eyes, the choroid was thinnest at the upper border of the staphyloma (mean, 37.4 μm; SD, 13.5 μm; range, 23–53 μm). Fluorescein angiography showed a band of window defects along the upper border of the staphyloma, where indocyanine green angiography demonstrated persistent hypoperfusion in all 5 eyes.

Conclusion: The choroid was markedly thin at the upper border of the inferior staphyloma accompanied by posterior serous retinal detachment. Such choroidal abnormality seemed to play an important role in the development of serous retinal detachment.

RETINA 32:1237–1242, 2012

Tilted disk syndrome is a congenital anomaly associated with malclosure of the embryonic optic fissure. Typical findings are inferonasal tilting of the disk, peripapillary crescent, myopia, staphyloma of the affected inferonasal region, thinning of retinal pigment epithelium (RPE) in the inferonasal fundus, or visual field defect.[1] These findings were often seen in bilateral eyes. In addition, some eyes without tilted disk also have inferior staphyloma and associated with chorioretinal change or degeneration.

In eyes with inferior staphyloma, macular complications such as choroidal neovascularization,[2] polypoidal choroidal vasculopathy,[3] or serous retinal detachment (SRD)[4–6] occasionally develop and impair the visual function when the upper border of the inferior staphyloma traverses the macula. However, the pathogenesis of these complications still remains unknown. Especially, SRD of this kind rarely shows spontaneous resolution. Although some previous studies have reported performing laser photocoagulation, this disorder turned out to be refractory to the laser treatment or, even if once resolved, sometimes showed postoperative redetachment.[4,6] About the pathogenesis, there may be some difference between SRD with inferior staphyloma and central serous chorioretinopathy (CSC), which is one of the most typical causes for posterior SRD.

Spaide et al[7] recently reported the enhanced depth imaging optical coherence tomography (EDI-OCT) method to acquire cross-sectional images of the

From the Department of Ophthalmology, Kyoto Prefectural University of Medicine, Kyoto, Japan.

Supported in part by Grant No. 21890226 from Ministry of Education, Culture, Sports, Science and Technology, Japan (Dr. H. Koizumi).

The authors declare no conflict of interest.

Reprint requests: Hideki Koizumi, MD, PhD, 465 Kajii-cho, Kamigyo-ku, Kyoto 602–0841, Japan; e-mail: hidekoiz@koto.kpu-m.ac.jp

choroid using a conventional spectral domain optical coherence tomography. This method improves the visualization of the intrachoroidal structure and chorioscleral interface. Using EDI-OCT, the choroidal thickness also can be measured.[8–11]

In this report, we performed EDI-OCT on eyes with posterior SRD associated with the inferior staphyloma for the purpose of providing new insights into the pathogenesis.

Patients and Methods

Retrospective analyses were performed on consecutive patients with SRD related to the inferior staphyloma. All patients underwent comprehensive ocular examinations including refractive error measurement, visual acuity testing using Landolt C charts, indirect slit-lamp biomicroscopy, color fundus photography, fluorescein angiography (FA), indocyanine green angiography (ICGA), and spectral domain optical coherence tomography.

Eyes with foveal SRD associated with the inferior staphyloma lying across the macula were included. Eyes were excluded if they had a history of previous intravitreal injection of any medication, a history of intraocular surgery or laser procedure (conventional laser photocoagulation, photodynamic therapy, or transpupillary thermotherapy), CSC, any type of choroidal neovascularization, any retinal vascular abnormalities, or use of any systemic or ocular corticosteroids. The EDI-OCT procedure was reported previously.[7] Briefly, the choroid was imaged by positioning the spectral domain optical coherence tomography (3D-OCT 1000 Mark II; Topcon Corp, Tokyo, Japan) device close enough to the eye to obtain an inverted image that automatically appears on the monitor to match those seen with conventional imaging. The 6-mm vertical scan, comprising a maximum of 16 averaged scans, was obtained through the center of the fovea of each eye. On this enhanced image, the choroidal thicknesses at the thinnest point around the macula, at the fovea, and at 0.5 mm and 1.0 mm superior and inferior to the thinnest point were measured perpendicularly to the RPE layers as the distance between the hyperreflective line corresponding to the outer surface of the RPE and the chorioscleral interface by use of the electronic caliper within the optical coherence tomography device. Fluorescein angiography and ICGA were performed with a confocal scanning laser ophthalmoscope (Heidelberg Retina Angiograph 2; Heidelberg Engineering, Dossenheim, Germany). Obtained images were correlated with the fundus photographs and the EDI-OCT images.

The choroidal thickness at each point was defined as the mean value of those measured by two independent observers. The paired *t*-test was used to evaluate the reproducibility of choroidal thickness measurement between the observers. Statistical analyses were performed using StatView software version 5.0 (SAS Institute, Inc, Cary, NC). A probability value of $P < 0.05$ was considered to be statistically significant.

The study protocol followed the tenets set forth in the Declaration of Helsinki, and ethics approval was obtained from the Institute Review Board of Kyoto Prefectural University of Medicine.

Results

There were five eyes of five patients diagnosed as having inferior staphyloma with SRD. All patients presented with visual loss and/or metamorphopsia. The mean age of the subjects was 50.2 years (SD, 21.5 years). Four of the five patients were women. The mean spherical equivalent was −3.4 diopters (SD, 2.0 diopters), and all eyes were phakic. Three of the five patients had bilateral tilted disk syndrome and bilateral inferior staphyloma; however, they had unilateral SRD. The other two eyes had unilateral inferior staphyloma and SRD without tilted disk syndrome.

The representative cases are shown in Figures 1 and 2. All five eyes biomicroscopically showed depigmentation of the RPE along the upper border of the staphyloma and SRD involving the center of the fovea. On the EDI-OCT images, the cross-sectional images of the choroid were visualized. In each of the five eyes, the upper border of the staphyloma traversed the macula and was located inferiorly to the foveal center. At the site of the upper border of the staphyloma, there was a finding of a markedly thin choroid. The average value of the choroidal thickness was 37.4 μm (SD, 13.4 μm; range, 23–53 μm) at the thinnest point around the macula and was 172.1 μm (SD, 44.7 μm; range, 110–219 μm) at the fovea. The characteristics and choroidal thicknesses of each case are summarized in Table 1. The choroidal thicknesses independently measured by the 2 observers were not significantly different ($P = 0.78$). The choroid became thicker superiorly and inferiorly to the thinnest point (Figure 3). On FA, a band of window defects were seen in all five eyes at the site of the RPE depigmentation observed under biomicroscopic examination. In three of the five eyes, FA demonstrated one or more focal active leaking sites inside the areas of the window defects. In the other two eyes, FA demonstrated no visible leaking sites. On the ICGA of all five eyes, an evident hypofluorescent band was

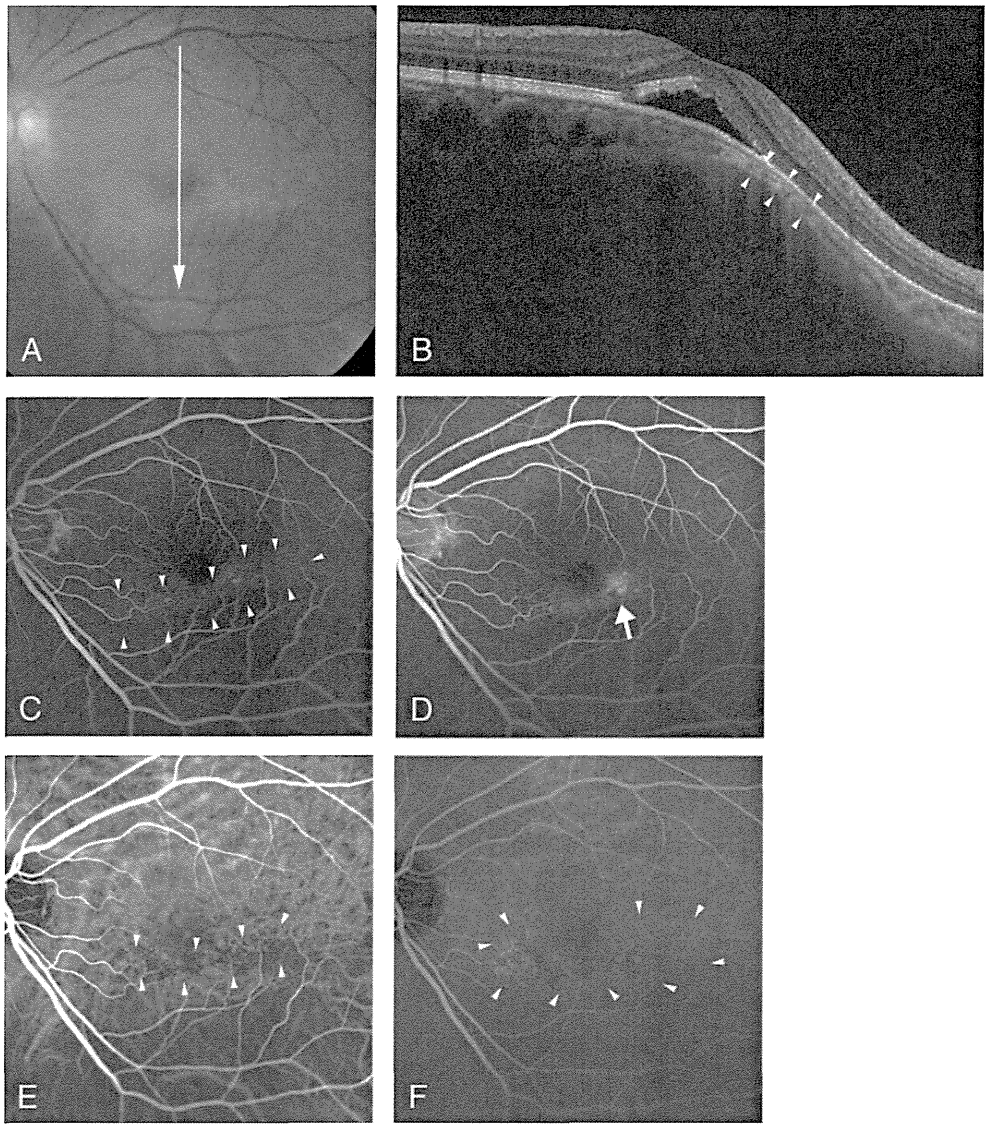

Fig. 1. Case 1. A 45-year-old woman with foveal retinal detachment associated with inferior staphyloma. The best-corrected visual acuity was 0.6 (decimal). **A,** Color fundus photograph of the left eye shows inferior staphyloma and foveal retinal detachment. Note that the upper border of the staphyloma lies across the macula. The arrow corresponds to a section examined with EDI-OCT. **B,** The vertical–sectional image through the fovea obtained with EDI-OCT displays subfoveal fluid and the markedly thin choroid (arrowheads) at the upper border of the staphyloma. The choroidal thickness at the thinnest point was 53 μm. **C,** The mid phase of FA demonstrates a band of window defects (arrowheads) corresponding to the upper border of the staphyloma. **D,** The late phase of FA reveals a focal leaking point in the parafoveal area (white arrow). **E,** The early phase of ICGA shows a hypofluorescent band (arrowheads). **F,** The late phase of ICGA demonstrates subtle hyperfluorescence (arrowheads) around the hypofluorescent band seen in the early phase.

detected corresponding to the areas of RPE depigmentation in the early phase and it was surrounded by subtle hyperfluorescence in the late phase.

Discussion

The findings of this study demonstrated marked thinning of the choroid at the upper border of the staphyloma associated with posterior SRD. The choroid appeared to be thicker superiorly and inferiorly to the thinnest point. This unique choroidal abnormality might have a relationship with the development of the SRD.

The upper border of the inferior staphyloma often traverses the macula. Cohen and Quentel[15] suggested that in eyes with tilted disk syndrome, the progression of the staphyloma may express upward traction on the RPE, the Bruch membrane, and the choriocapillaris complex from the upper border of the staphyloma. Although speculative, the upward traction superior to this border might possibly be related to anatomical changes of RPE (RPE atrophy) and choroid (choroidal thinning).

In the present study, EDI-OCT revealed a very thin choroid of 37.4 μm on average at the upper border of the staphyloma. By means of EDI-OCT, it was reported that the subfoveal choroidal thickness was 287 μm in healthy eyes[9] and 93.2 μm in highly myopic eyes.[8] Accordingly, in our cases, the choroidal thickness at the upper border of staphyloma was much less than that at the fovea in healthy eyes and even less than that in highly myopic eyes.

Although several reports have been published about this disorder, the detail of the pathogenesis

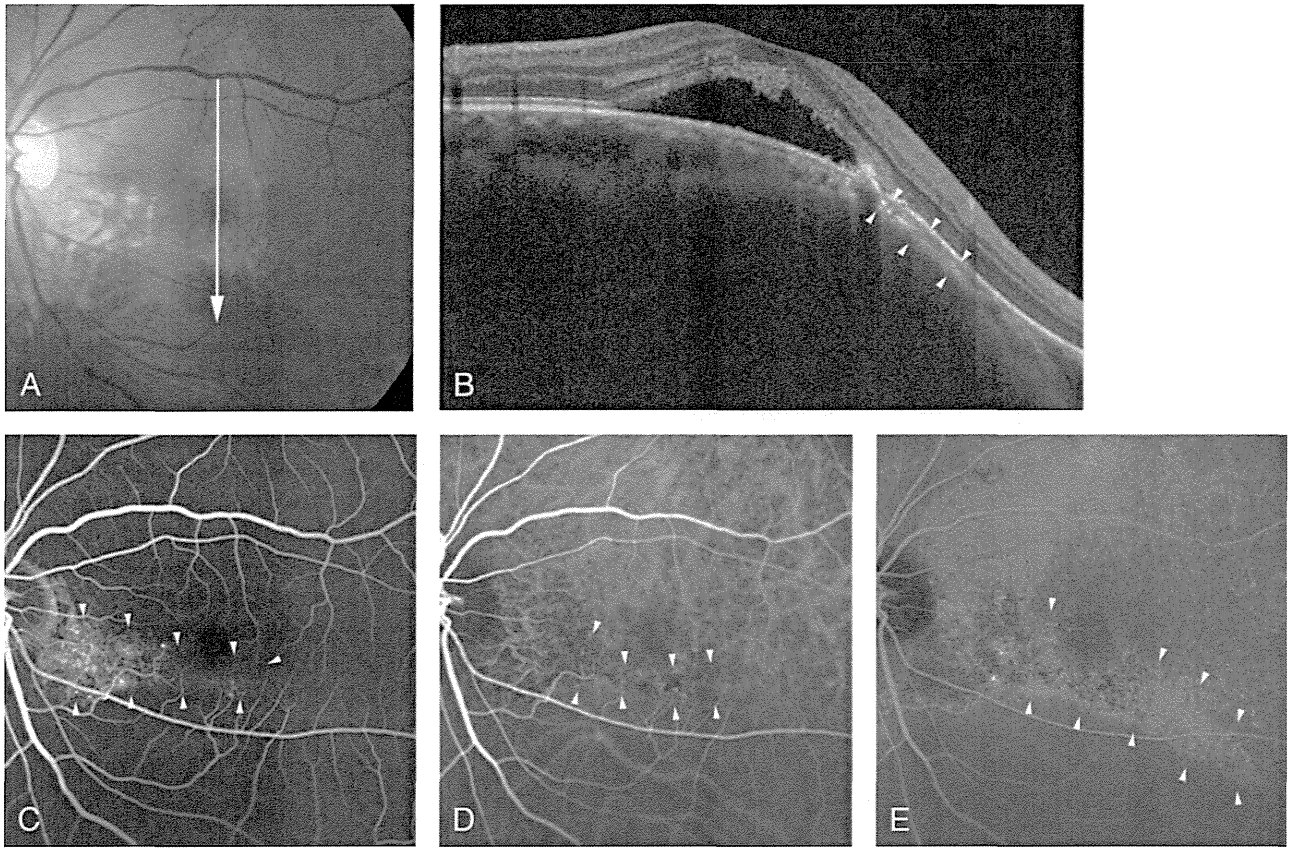

Fig. 2. Case 3. A 44-year-old woman with foveal retinal detachment associated with inferior staphyloma. The best-corrected visual acuity was 1.2 (decimal). **A,** Color fundus photograph of the left eye shows inferior staphyloma with SRD involving the fovea. The upper border of the staphyloma traversed the macula. The arrow indicates a section examined with EDI-OCT. **B,** The vertical–sectional image through the fovea obtained with EDI-OCT demonstrates subretinal fluid and a markedly thin choroid (arrowheads) at the upper border of the staphyloma. The choroidal thickness at the thinnest point was 23 μm. **C,** The mid phase of FA shows a band of window defects (arrowheads) along the upper border of the staphyloma. This case showed no active leakage in all phases of FA. **D,** The early phase of ICGA demonstrated hypofluorescent band (arrowheads). **E,** The late phase of ICGA showed subtle hyperfluorescence (arrowheads) around the hypofluorescent band seen in the early phase.

remains unclear. Cohen et al[4] and later Leys and Cohen[6] described FA findings in tilted disk syndrome with posterior SRD and mentioned that not only RPE dysfunction but also anomalies of the choroidal perfusion at the upper border of the staphyloma could explain the SRD. This theory could be supported by an experimental study by Yao and Marmor[16] who demonstrated that in rabbit eyes, RPE damage alone was not sufficient to cause SRD; however, both RPE and the choriocapillaris should be impaired to induce SRD. In the same study, it was also proved that SRD spontaneously resolved when the choriocapillaris was not damaged, even in the absence of RPE. Therefore, the choroid appeared to play a key role in the accumulation and resorption of SRD rather than RPE. There is a direction of flow from the vitreous to the choroid, and the latter acts as a means of fluid resorption. All five cases in the present study showed both RPE atrophy and a very thin choroid at the upper border of the inferior staphyloma. The decreased ability of the choroid to remove the SRD may be responsible, at least in part, for the development of posterior SRD.

Nakanishi et al[17] reported the pathophysiology of tilted disk syndrome with macular complications including SRD. In their study, the hypofluorescent area was seen at the upper border of the staphyloma in the early phase of ICGA, later surrounded by hyperfluorescence seen in the late phase. They hypothesized that the hyperfluorescence might indicate choroidal vascular hyperpermeability, which was also previously reported to be seen in eyes with CSC,[12–14] probably induced by a possible mechanical force or hemodynamic change. The choroid in eyes with CSC was markedly thick compared with that of normal eyes.[11] Our cases also revealed ICGA findings similar to those shown by Nakanishi et al, but the EDI-OCT images obtained in our study demonstrated apparent thinning

Table 1. Characteristics and Choroidal Thicknesses of the Patients with Foveal SRD Associated with Inferior Staphyloma

Case	Gender	Eye	Age (Years)	BCVA (Decimal)	Spherical Equivalent (D)	Choroidal Thickness at the Thinnest Point (μm)	Subfoveal Choroidal Thickness (μm)
1	F	L	45	0.6	−2.0	53	166
2	F	R	25	1.0	−5.0	46	219
3	F	L	44	1.2	−1.5	23	212
4	M	L	84	0.3	−2.5	42	110
5	F	L	53	1.0	−6.0	25	155
Mean choroidal thickness						37.4 ± 13.4 (SD)	172.1 ± 44.7 (SD)

BCVA, best-corrected visual acuity; D, diopters; F, female; L, left eye; M, male; R, right eye.

of the choroid at the upper border of the staphyloma. Thus, we believe that the pathogenesis of SRD seen in our cases might be somewhat different from that of CSC.

The present study had several limitations. The number of cases was limited. The images of the EDI-OCT were obtained in a single line, and the choroidal thickness measurement did not cover the overall macular area. Although the use of EDI-OCT allowed for the subfoveal choroidal thickness to be evaluated with a lesser number of images than previously reported,[7] the optical coherence tomography used in this study did not include the eye tracking system and thus may present a weakness in obtaining images with the best contrast. This study was only a cross-sectional study, and the follow-up period was limited. Thus, further studies are required to elucidate the pathogenesis of the disorder.

In conclusion, the findings of the study showed the marked thinning of the choroid at the upper border of the staphyloma in eyes with posterior SRD associated with inferior staphyloma. At the same lesion, the hypofluorescent finding on ICGA was evident. Both the RPE dysfunctions and the choroidal circulatory disturbances might possibly be attributed to the pathogenesis of SRD.

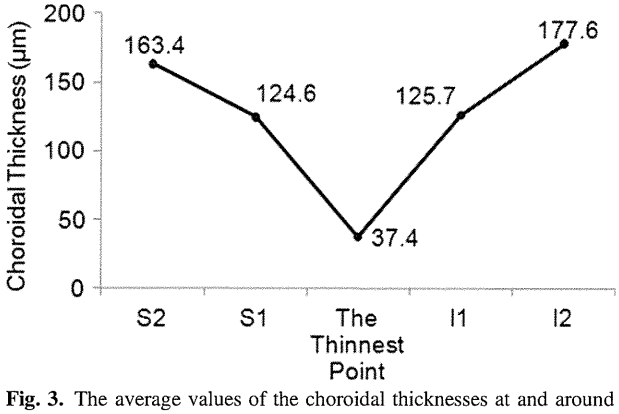

Fig. 3. The average values of the choroidal thicknesses at and around the thinnest point. The choroid was relatively thick at the superior and inferior sites compared with the thinnest point; S1, 0.5 mm superior; S2, 1.0 mm superior; I1, 0.5 mm inferior; I2, 1.0 mm inferior to the thinnest point. The numbers adjacent to the plotted points shown in the graph represent the averaged choroidal thicknesses at each point.

Key words: tilted disk syndrome, inferior staphyloma, serous retinal detachment, optical coherence tomography, enhanced depth imaging optical coherence tomography (EDI-OCT), choroid, choroidal thickness, retinal pigment epithelium.

References

1. Apple DJ, Rabb MF, Walsh PM. Congenital anomalies of the optic disc. Surv Ophthalmol 1982;27:3–41.
2. Tsuboi S, Uchihori Y, Manabe R. Subretinal neovascularisation in eyes with localised inferior posterior staphyloma. Br J Ophthalmol 1984;68:869–872.
3. Mauget-Faysse M, Cornut PL, Quaranta El-Maftouhi M, Leys A. Polypoidal choroidal vasculopathy in tilted disk syndrome and high myopia with staphyloma. Am J Ophthalmol 2006;142:970–975.
4. Cohen SY, Quentel G, Guiberteau B, et al. Macular serous retinal detachment caused by subretinal leakage in tilted disc syndrome. Ophthalmology 1998;105:1831–1834.
5. Tosti G. Serous macular detachment and tilted disc syndrome. Ophthalmology 1999;106:1453–1455.
6. Leys AM, Cohen SY. Subretinal leakage in myopic eyes with a posterior staphyloma or tilted disk syndrome. Retina 2002; 22:659–665.
7. Spaide RF, Koizumi H, Pozzoni MC. Enhanced depth imaging spectral-domain optical coherence tomography. Am J Ophthalmol 2008;146:496–500.
8. Fujiwara T, Imamura Y, Margolis R, et al. Enhanced depth imaging optical coherence tomography of the choroid in highly myopic eyes. Am J Ophthalmol 2009;148:445–450.
9. Margolis R, Spaide RF. A pilot study of enhanced depth imaging optical coherence tomography of the choroid in normal eyes. Am J Ophthalmol 2009;147:811–815.
10. Spaide RF. Enhanced depth imaging optical coherence tomography of retinal pigment epithelial detachment in age-related macular degeneration. Am J Ophthalmol 2009; 147:644–652.
11. Imamura Y, Fujiwara T, Margolis R, Spaide RF. Enhanced depth imaging optical coherence tomography of the choroid in central serous chorioretinopathy. Retina 2009;29: 1469–1473.